ISTANBUL TECHNICAL UNIVERSITY ★ GRADUATE SCHOOL OF SCIENCE ENGINEERING AND TECHNOLOGY

IMPLEMENTATION OF FLUCTUATING PRESSURE MEASUREMENTS IN A SUPERSONIC INLET AT ITU TRISONIC WIND TUNNEL

M.Sc. THESIS

Hasan TABANLI

Department of Aeronautical and Astronautical Engineering

Aeronautical and Astronautical Engineering Programme

JANUARY 2014

ISTANBUL TECHNICAL UNIVERSITY ★ GRADUATE SCHOOL OF SCIENCE ENGINEERING AND TECHNOLOGY

IMPLEMENTATION OF FLUCTUATING PRESSURE MEASUREMENTS IN A SUPERSONIC INLET AT ITU TRISONIC WIND TUNNEL

M.Sc. THESIS

Hasan TABANLI
(511091161)

Department of Aeronautical and Astronautical Engineering

Aeronautical and Astronautical Engineering Programme

Thesis Advisor: Asst. Prof. Dr. K. Bülent YÜCEİL

JANUARY 2014

İSTANBUL TEKNİK ÜNİVERSİTESİ ★ FEN BİLİMLERİ ENSTİTÜSÜ

İTÜ TRİSONİK RÜZGAR TÜNELİNE SESÜSTÜ HAVA ALIĞINDA ÇALKANTILI BASINÇ ÖLÇÜMLERİ KABİLİYETİNİN KAZANDIRILMASI

YÜKSEK LİSANS TEZİ

Hasan TABANLI
(511091161)

Uçak ve Uzay Mühendisliği Anabilim Dalı

Uçak ve Uzay Mühendisliği Programı

Tez Danışmanı: Yard. Doç. Dr. K. Bülent YÜCEİL

OCAK 2014

Hasan TABANLI, a M.Sc. student of ITU Graduate School of Science Engineering and Technology 511091161 successfully defended the thesis entitled **"IMPLEMENTATION OF FLUCTUATING PRESSURE MEASUREMENTS IN A SUPERSONIC INLET AT ITU TRISONIC WIND TUNNEL"**, which he prepared after fulfilling the requirements specified in the associated legislations, before the jury whose signatures are below.

Thesis Advisor :	**Yard. Doç. Dr. K. Bülent YÜCEİL** İstanbul Teknik Üniversitesi	.....
Jury Members :	**Yard. Doç. Dr. K. Bülent YÜCEİL** İstanbul Teknik Üniversitesi	.....
	Yard. Doç. Dr. Hayri ACAR İstanbul Teknik Üniversitesi	.....
	Doç. Dr. Mustafa ÖZDEMİR İstanbul Teknik Üniversitesi	.....

Date of Submission : **16 December 2013**
Date of Defense : **23 January 2014**

To my wife,

FOREWORD

Firstly, I would like to express my deepest gratitude to my supervisor Asst. Prof. Dr. K. Bülent YÜCEİL for giving me the opportunity to join his research group to conduct this study. I appreciate his guidance, support and creative suggestions throughout this study. I truly thankful for his patience and encouragement to finish my work. It was a great honor to work with him on my thesis.

I am especially grateful to Asst. Prof. Dr. Hayri ACAR, Asst. Prof. Dr. Duygu ERDEM, Prof. Dr. N. L. Okşan ÇETİNER-YILDIRIM and Dr. İdil FENERCİOĞLU; for their valuable help, advice and friendship. I feel lucky that I had the chance to work with them.

With their self-sacrificing support, I would like to express my gratitude to my colleagues Res. Asst. Ali EKEN, Res. Asst. Onur SON, Res. Asst. Banu YILMAZ, Res. Asst. Seher EKEN, Res. Asst. Serhat YILMAZ and Serdar SEÇKİN for their sense of humor and support.

I would also like to thank the technicians of Trisonic Research Laboratory, Murat TARHAN and Aliosman TABANLI, for their cooperation. I especially extend my thanks to Aliosman TABANLI because admittedly without his devotion this thesis would never be completed.

Above all, I would like to thank my mother, my father and my sister. I could not achieve anything without them.

At last but at most, I would like to thank to my wife Sevcan TABANLI for her great love, patience, guidance and support during my life and this study. Furthermore I appreciate her editorial help. Her existence encouraged me to carry on through the thick and thin.

January 2014 Hasan TABANLI

TABLE OF CONTENTS

Page

ABBREVIATIONS

$\mathbf{A}_{ts}$	**:** Throat area required to start the inlet
$\mathbf{A}_{tr}$	**:** The throat area required at normal operation
$\mathbf{C}_R$	**:** Correction factor
$\mathbf{F}_n$	**:** Net Thrust
M	**:** Mach number
$\mathbf{P}_m$	**:** Mean pressure
$\mathbf{P}_t$	**:** Total pressure
$\mathbf{P}_\infty$	**:** Free-stream pressure
T	**:** Transducer
$\boldsymbol{\sigma}_p$	**:** Quadratic mean of pressure

LIST OF TABLES

Page

LIST OF FIGURES

Page

IMPLEMENTATION OF FLUCTUATING PRESSURE MEASUREMENTS IN A SUPERSONIC INLET AT ITU TRISONIC WIND TUNNEL

SUMMARY

The inlet is the first component on the aircraft engine and interacts directly with the ambient atmosphere. The primary purpose of the inlet is to bring the air required by the engine from freestream conditions to the conditions required at the entrance of the fan or compressor. Turbojet and turbofan engines are incapable of efficient operation unless the air entering them is slowed down to a speed of about Mach 0.4-0.5. This is to keep the tip speed of the compressor blades below sonic speed relative to the incoming air.

In air inlets, undesirable adverse events such as decrement in flow capture, increment in spillage drag and even unstart situation may occur during the flight. Since the 60s, many experimental and computational studies have been performed to better understand the flow conditions in the supersonic air inlets. Also in recent years at our country various supersonic aircraft projects being carried out and these studies are encouraged by the Ministry of National Defense.

In this thesis, it is aimed to gain a capability for and to perform unsteady and fluctuating surface pressure measurements in the ITU Trisonic Wind Tunnel for complex flow problems in a supersonic inlet model. The goal required to develop means to use miniature surface pressure transducers and also to make modifications on the tunnel test section floor, which had not been attempted since the procurement of the wind tunnel at the University.

To perform the pressure measurements Kulite-brand miniature transducers were used due to their satisfactory performance at dynamic pressure measurements as well as their small size. A calibration unit were designed and manufactured to calibrate the transducers for their output voltage in order to obtain the maximum signal resolution for data acquisition.

Kulite transducers used in the study do not come with any sort of mounting means such as a screw thread or a similar mechanism to mount them flush with the surface. Special holder-sleeves with outer threads have been designed and manufactured both to protect the transducers from mechanical damage and to enable them to be re-installed in a given port on the pressure-measurement plug.

The wind tunnel test section floor was modified to accommodate a pressure-measurement plug with 35 holes for installing the transducers flush with the surface in minimum of 5 mm intervals. The plug was produced and assembled to the floor of the test section which also forms the bottom wall of the inlet model. A supersonic inlet model with a sharp-edged shock generator (a 12-degree compression ramp) was manufactured and mounted to the test section floor.

Experiments were carried out in the 150 x 150 mm Trisonic Wind Tunnel located at Istanbul Technical University. First, schlieren and shadowgraph imaging methods were

used to determinate the shock wave pattern and structure in and around the inlet model. The schlieren image revealed that the internal shock structure of the inlet consisted of an initial ramp shock and three reflected shock waves. Schlieren imaging also showed that these shock waves interacted with the boundary layer developing on the surface of the tunnel floor and formed regions of shock wave boundary layer interaction and flow separation. Using the information gained from these observations locations of the pressure transducers were determined to obtain the pressure distribution and to study the shock boundary layer interaction over the floor of the inlet model. Following flow visualization experiments, fluctuating pressure measurements were performed on the floor of the inlet model at Mach 2. Pressure data were acquired at rates of 200 kHz and 40 kHz and normalized by the freestream static pressure which was measured by a transducer located slightly upstream of the inlet.

In the first case, the influence of the shock wave/boundary layer interaction occurring on the floor caused by the impingement of the ramp oblique shock on the pressure along the wall was observed by the first upstream transducer within the inlet, which had higher pressure fluctuations than those of other transducers downstream. In the second case, upstream extent of the interaction caused by the ramp shock was determined by performing the pressure measurements in the upstream portion of the inlet at the highest spatial resolution by placing the transducers adjacent to each other. In the third case, an attempt to investigate the details of the third reflection of the ramp shock wave and the related issues which were observed in the flow visualization results has been made by performing pressure measurements in the downstream portion of the inlet again with the highest spatial resolution configuration of transducers.

This study constitutes a milestone for more comprehensive and advanced studies of flow in and around inlets and inlet unstart which might result from shock wave boundary layer interactions and boundary layer separations.

İTÜ TRİSONİK RÜZGAR TÜNELİNE SESÜSTÜ HAVA ALIĞINDA ÇALKANTILI BASINÇ ÖLÇÜMLERİ KABİLİYETİNİN KAZANDIRILMASI

ÖZET

Bir uçak motorun serbest çalışma şartlarına göre uçağa takıldıktan sonraki performans azalması büyük oranda hava alığı sistemine bağlı olarak değişmektedir. Hava alığı giriş ve iç geometrik özellikleri motora sağlanan hava akışında basınç kaybı ve düzgün akış şartlarını bozma etkileri göstermektedir: % 1'lik basınç kaybı (motora giren hava akışının toplam basıncı/alığa yaklaşan hava akışının toplam basıncı) motor itkisinde yaklaşık % 1.3 azalmaya neden olmaktadır. Bunun yanında hava alığının dış geometrisi ve sınır-tabaka uzaklaştırıcı sistemler de uçağın sürükleme kuvvetini arttırıcı ve performansını azaltıcı etki oluşturmaktadır.

Yüksek sesaltı ve sesüstü hıza sahip uçaklarda kullanılan turbojet ve turbofan motorların verimli çalışabilmeleri için girişte 0.4 ve 0.5 Mach arasında hava akışıyla beslenmeleri gerekmektedir. Bu hızdan yüksek hava akışında kompresör palalarında şok dalgaları oluşmakta ve verim aniden düşmektedir. Sesten hızlı uçaklardaki hava soluyan motorlarda kullanılan hava alıkları, motora giren sesüstü akışı uygun şekilde yavaşlatmaya yarayan şok dalgaları üretecek bir geometrik yapıya sahip olacak şekilde tasarlanırlar. Sesüstü hızlar için tasarlanan hava alıklarında akış şartlarını olumsuz yönde değişime uğratan birçok etken bulunmaktadır.

Hava alığının ürettiği şok dalgalarının, alığın tasarım şartları dışındaki akış ve çalışma şartlarında ya da kompresör veya yanma odası şartlarındaki değişimlerden kaynaklanan etkiler nedeniyle alık dışına taşması (unstart) bu tip motorlarda karşılaşılan ciddi problemlerden birisidir. Alık başlamama olarak da adlandırılan bu durum özellikle motor susması gibi çok olumsuz sonuçlara yol açabilmektedir.

Sesüstü hava alıklarında oluşan dik ya da güçlü şok dalgaları alık yüzeyinde gelişen sınır tabaka için oldukça ters bir basınç gradyanı oluşturarak etkileşime girer. Bu etkileşim geniş ölçekli bir sınır tabaka ayrılmasına yol açmasının yanında sesüstü hava alıklarının akış yakalama ve kayıp (flow capture and loss) karakteristikleri, taşma sürüklemesi (spillage drag), sınır tabaka atma (bleed) tasarımı ve alık akış kararsızlığı ya da 'buzz' olarak bilinen problemin ortaya çıkma önceliğini (onset) etkilemesi açısından önemli sonuçlar doğurabilmektedir. Şok dalgası sınır tabaka etkileşimleri ve başlamamış alık problemleri çok çeşitli geometri ve şartlarda yoğun olarak 60'lı yıllardan beri yapılan birçok deneysel ve hesaplamalı çalışma ile incelenmektedir. Önceki yıllarda yapılan çalışmalar daha çok etkileşimin zaman ortalaması (mean) sonuçlarını ortaya koyarken son yıllarda etkileşimin zamana bağlı ve yapısal/malzeme açısından yorulma ve kırılmalara yol açan yönü incelenmektedir. Ülkemizde de son yıllarda sesüstü hızlarda görev yapmak üzere tasarlanan ve üretilmesi planlanan çeşitli uçak projeleri yürütülmekte ve bu çalışmalara Milli Savunma Bakanlığı tarafından destek verilmektedir.

Bu tez çalışmasında, sesüstü hava alığında oluşan şok dalgalarının alık yüzeyinde neden olduğu basınç dağılımının ve alık içindeki şok dalgalarının sınır tabaka ile etkileşimi sonucu ortaya çıkan zamana bağlı yüzey basınç değişimlerinin elde edilmesi amacıyla İTÜ Uçak ve Uzay Bilimleri Fakültesindeki 150 x 150 mm Trisonik Rüzgar Tünelinde zamana bağlı (çalkantılı) yüzey basınç ölçümleri yapabilme yeteneği ve kapasitesi kazanılması ve sesüstü bir alık modelinde bu ölçümlerin yapılarak sonuçların irdelenmesi hedeflenmiştir.

Basınç ölçümleri için yüksek frekans cevabı olan ve rüzgar tüneli testleri için üretilmiş olan "Kulite" marka minyatür basınç duyargaları kullanılmıştır. Ancak bu duyargalar ilgili basınç aralıkları içinde kullanıcı tarafından farklı basınç şartlarında kullanılabilmektedir. Bu sebeple ölçümlerden önce basınç duyargalarına kullanılacakları basınç aralığına göre kalibrasyon işlemi uygulanmıştır. Bu amaçla içine duyargaların yerleştirilebildiği, rüzgar tünelinde sesüstü hızlarda serbest akımda karşılaşılan düşük basınçlardan, şok arkası yüksek basınçlara kadar olan aralıklarda belirli statik basınç değerlerinin uygulanabildiği sızdırmaz bir kap tasarlanıp üretilmiştir. Sızdırmaz kap, yüksek hassasiyete sahip analog göstergeli bir basınç ölçer, vakum pompası, basınç pompası, güç kaynağı ve veri toplama kartı barındıran bilgisayar uygun şekilde bir araya getirilerek bir kalibrasyon ünitesi üretilmiştir. LabView ortamında hazırlanan bir kod kullanılarak gerekli basınç aralıklarında duyargaların kalibrasyonu yapılmıştır.

Basınç ölçümlerinde kullanılacak olan duyargalar 9.5 mm uzunluğunda ve 1.85 mm çapında silindir geometrisine sahip, oldukça hassas cihazlar olduğundan model yüzeylerine takılabilmesi için koruyucu ve vidalama özelliği olan uygun bir adaptör içine yerleştirilmeleri gerekmektedir. Bu amaçla içi buna uygun çapta delinmiş dışı M3 dişe sahip adaptörler üretilmiş ve özel bir montaj tekniği ile duyargalar ile birleştirilmiştir. Ayrıca model yüzeyinde duyarganın yeri değiştirilmek veya çıkarılmak istendiğinde, basınç ölçüm portlarından o anda kullanılmayanları kapamak amacıyla özel tıpalar üretilmiştir.

Trisonik Rüzgar Tünelini deney odasının alt duvarı aynı zamanda hava alığı modelinin alt duvarını da oluşturmakta ve hava alığının ürettiği ilk şok dalgası bu yüzeye çarpıp yansımaktadır. Bu yüzeyde farklı noktalarda basınç ölçümlerinin yapılabilmesi için 5 mm aralıklarla toplam 35 adet basınç ölçüm portuna sahip bir ara parça imal edilmiş ve rüzgar tüneli deney odasının alt duvarı bu ara parçaya uygun şekilde yeniden tasarlanarak üretilmiştir.

Ölçüm altyapısının kurulması sürecinde bu altyapının en verimli şekilde test edilmesi amacıyla kama/rampa şekilli keskin kenarlı bir şok dalgası üretecine sahip hava alığı tasarlanıp üretilmiştir. Üretilen model kullanılarak Schlieren yöntemi ile akım görünürlüğü deneyi yapılmıştır. Schlieren düzeneğinde bıçak sırtı yatay konumda tutularak şok dalgalarının yanı sıra model yüzeylerinde gelişen sınır tabakanın da daha belirgin hale getirilmesi amaçlanmıştır. Akım görüntüleme deneylerinin sonucunda alık girişinde oluşan eğik şok dalgasının alık iç yüzeyinde birkaç yansımaya neden olduğu ve üçüncü yansımanın alık dışına çıktığı gözlenmiştir. Schlieren görüntülerinden faydalanılarak duyargaların hangi portlara konumlandırılacakları belirlenmiştir. Bu akış şartında ortaya çıkan zamana bağlı basınç değişimleri yüzeye pürüzsüz olarak yerleştirilmiş olan 7 adet duyarga ile ölçülmüştür. Söz konusu ölçümlerde LabView ortamında hazırlanan bir kod kullanılmıştır. Alınan basınç verisi istatistiksel yöntemlerle analiz edilerek ortalama basınç dağılımları, basınç

değişimlerindeki öne çıkan salınım frekansları elde edilerek alık içindeki sesüstü akışın yapısı ve özellikleri elde edilmiştir.

Bu tez kapsamında yapılan donanım ve yazılım çalışmalarının sonucunda Trisonik Rüzgar Tüneli hava alık modelleri içinde dinamik basınç ölçümleri yapabilme kabiliyeti kazanmıştır. İleriki çalışmalarda da bu şekilde elde edilecek olan konumsal ve zamana bağlı basınç değişimleri alık içerisindeki karmaşık akışın daha iyi anlaşılmasında, alık başlamama problemini tetikleyen şartların belirlenmesinde ve şok dalgalarının sınır tabaka ile etkileşimi sonucu ortaya çıkan akış şartlarının tespit edilmesinde çok önemli katkılar sağlayacaktır.

1. INTRODUCTION

A supersonic aircraft is designed to exceed the speed of sound in at least some of its normal flight configurations. Supersonic flight brings with it substantial technical challenges, as the aerodynamics of supersonic flight are dramatically different from those of subsonic flight. These challenges have largely been met since 1950s. However, supersonic aircrafts are still open to development.

Supersonic aircraft are affected by shock waves which are prime importance in air intakes whose purpose is to provide a stable, uniform, low-loss, subsonic flow to the engine face at all flight conditions. Inlet design is highly complex due to the requirement to manage flow and shock formation through the supersonic flight regimes. Oblique shock waves are an efficient form of compression; however, they interact with the boundary layer forming on the inlet walls. The shock-induced adverse pressure gradient can trigger large-scale separation, resulting in significant total pressure loss and flow distortion. Furthermore, the unsteady aspects of separated shock-wave/boundary-layer interactions can cause large structural loads and may even lead to inlet unstart. It is therefore beneficial to understand the flow either before or during the interaction process.

The need for supersonic aircraft in our country have been indispensable particularly in the military. For that reason in recent years at our country various supersonic aircraft projects being carried out and these studies are encouraged by the Ministry of National Defense. In determining the goals of this study, these developments were taken into account.

The objective of this study is to gain a capability to perform unsteady and fluctuating pressure measurements in the Trisonic Wind Tunnel. The development of the Trisonic Wind Tunnel is also important because of having the largest test section area for supersonic conditions in Turkey.

This thesis is instructive study for instrumentation of the wind tunnel to perform fluctuating pressure measurements in a supersonic inlet model.

In the first part of thesis some basic concepts about supersonic inlets are briefly explained. The wind tunnel instrumentation to measure fluctuation pressure has described in the experimental part. In the conclusion, the flow visualization and pressure measurement results for basic supersonic inlet has given.

2. BASIC CONCEPTS ABOUT SUPERSONIC INLETS

The inlet is the first component on the engine and interacts directly with the ambient atmosphere. The primary purpose of the inlet is to bring the air required by the engine from free-stream conditions to the conditions required at the entrance of the fan or compressor. The performance of an inlet is related to the following characteristics:

- Handle a wide range of mass flow
- Duct air to the engine with low total pressure loss and low drag
- Diffuse the flow over its length to high pressure and low Mach number
- Minimize distortions in the flow field exiting the inlet
- Low weight, small size, and mechanically simple

Supersonic inlets are classified into three basic types, characterized by the location of the supersonic compression wave system: internal compression, external compression, and mixed compression.

2.1 Internal Compression Inlets

The internal compression inlet is shown in Figure 2.1. In this inlet a pair of inward-facing ramps produce a series of internal oblique shock waves followed by a terminal normal shock positioned downstream of the throat at its stable location [1].

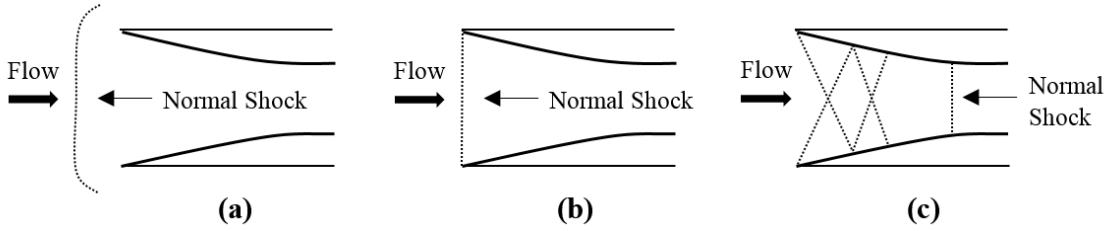

Figure 2.1: Internal compression inlet (a) Unstarted inlet, (b) Inlet starting, (c) Normal operation

Weakness of this type inlet is that any deviation in flow condition, such as temperature, pressure, or angle of attack can cause movement of the terminal shock to across the

inlets front. This leads to inlet unstarting (Figure 2.1(a)) due to the total internal flow pattern corruption. This unstarted condition of the inlet can also occur by bringing the free-stream Mach number from subsonic up to design Mach number without changing the throat area sufficiently to start the inlet. This type of inlet requires variable throat area to allow the inlet to swallow the normal shock during starting. Fast reaction bypass doors are also required downstream of the throat to permit proper positioning of the normal shock under varying flight and engine conditions. When the normal shock forms ahead of the inlet as shown in Figure Figure 2.1(a) it induces low total pressure ratio, reduced mass flow through the inlet, high spillage drag, and possible engine flameout [1].

For the internal compression inlet, the ratio of the throat area required to start the inlet A_{ts} to the throat area required at normal operation A_{tr} is expressed by Mattingly [1] and plotted in Figure 2.2.

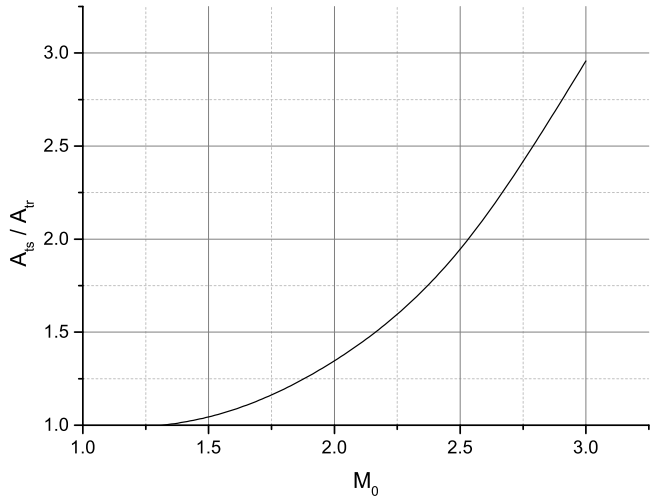

Figure 2.2: Throat area variation required of an internal compression inlet

This large area variation to start the inlet at Mach numbers greater than 2, the problem of inlet unstart, the poor performance at angles of attack, and some other problems have led to the demise of the internal compression inlet.

2.2 External Compression Inlet

The compression in the external compression inlet is achieved through either one or a series of oblique shocks followed by a normal shock or simply through one normal shock.

2.2.1 Single Normal Shock Inlets

The normal shock inlet is simply a forward-facing hole. It is simple, short, lightweight, inexpensive and commonly used at low supersonic speeds. It is also called a *"pitot inlet"* when used for subsonic flight is shown in Figure 2.3.

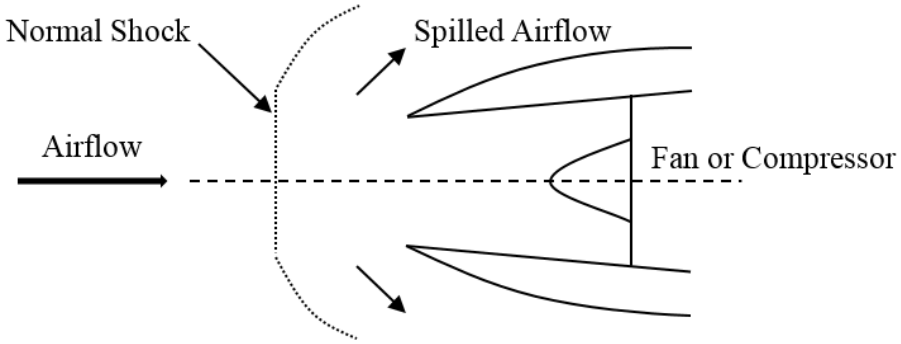

Figure 2.3: Pitot or normal shock inlet

Engine performance and aircraft drag are significantly affected by cowl lip radius. When the speed of sound is approached, a large lip radius will produce shock-separated flow on the outside of the inlet and that dramatically increases the drag. Therefore the cowl lip should be nearly sharp for supersonic jets [2].

The inlet front face may not be perpendicular to the engine axis. The location of the inlet and the aircraft's angleofattack range are decisive on the front-face orientation. Normally the inlet should be about perpendicular to the local flow direction during cruise. If the aircraft is to operate at large angles of attack, it may be desirable to compromise between these angles and the angle at cruise [2].

It is necessary that the shock be situated at the inlet lip in order to have the maximum possible mass flow enter the inlet under supersonic flight conditions. The shock wave increases the pressure by compression that drops the Mach number to subsonic levels; as the flow proceeds through the expanding area of the duct, the pressure increases. This is shown schematically in Figure 2.4.

Although the shock wave causes increment on the static pressure, but the effect of the shock wave also decreases the stagnation pressure. The stagnation pressure loss in the inlet is crucial to overall engine performance. The stagnation pressure recovery for a normal shock inlet is shown in Figure 2.5.

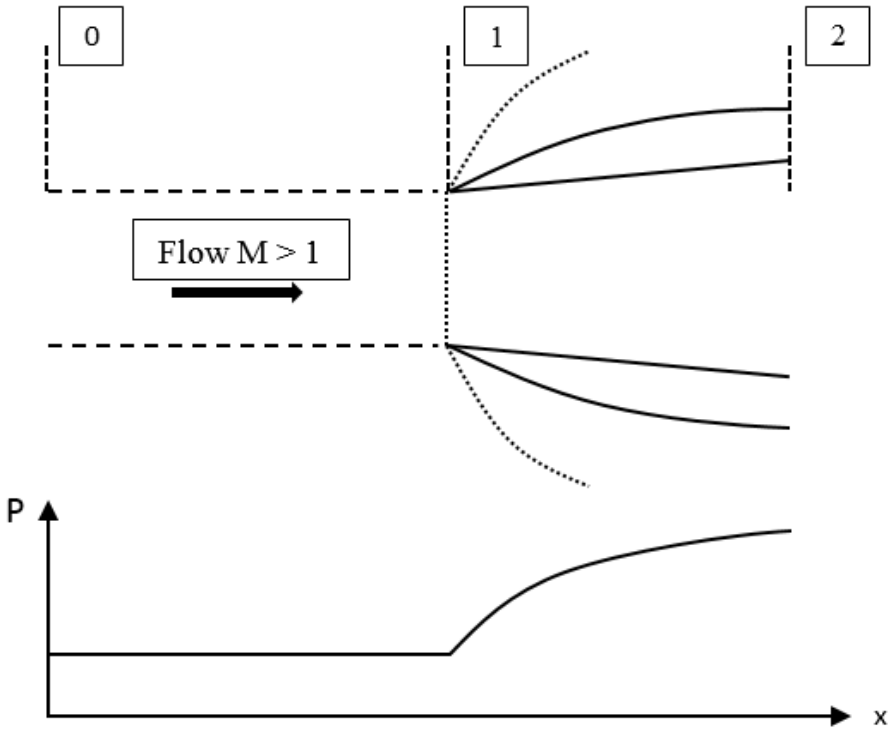

Figure 2.4: Normal shock inlet in supersonic flight showing shock placement for maximum inlet mass flow

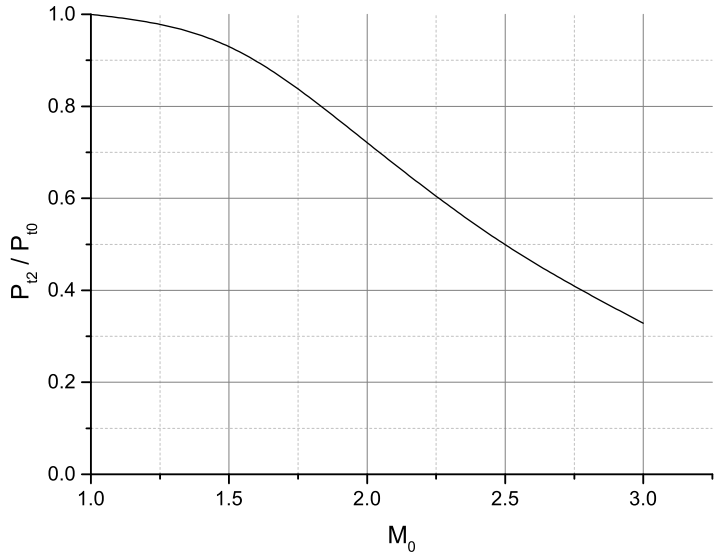

Figure 2.5: Total pressure recovery for normal shock inlets (normal shock at the inlet lip) as a function of flight Mach number

The performance of such an inlet is directly proportional to the stagnation pressure at station 2, $p_{t,2}$. In addition, the exhaust velocity, and therefore the net thrust per unit mass flow, is also proportional to $p_{t,2}$. Hesse and Mumford [3] proposed the normalized change in net thrust due to inlet losses as follows:

$$\frac{\Delta F_n}{F_n} = -(1 - \frac{P_{t,2}}{P_{t,0}})C_R$$

The correction factor C_R is in the range of 1.1 and 1.6 according to Antonatas et al. [4]. The general behavior shown in Figure2.6 is for an average value of C_R = 1.35 in order to provide a reasonable estimate of the performance loss attributable to using a normal shock inlet in supersonic flight. It is apparent from Figure 2.6 that the normal shock inlet is satisfactory at Mach numbers up to about M= 1.5, especially since it is a very simple and robust device. However, above this Mach number another more efficient inlet design must be used because the losses become dramatically great to justify its use.

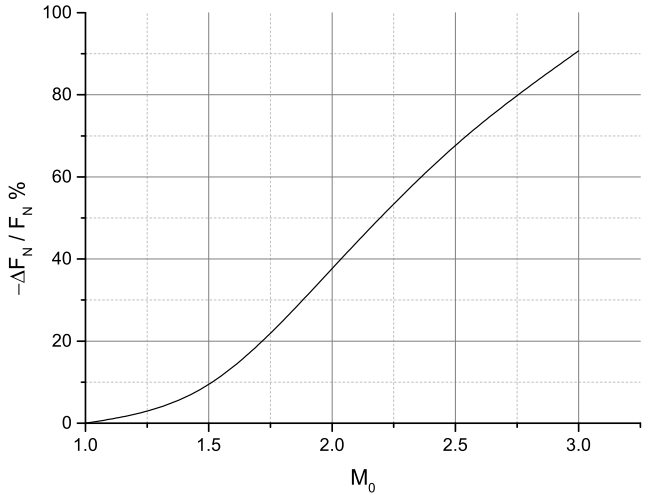

Figure 2.6: Nominal reduction in net thrust as a function of Mach number for normal shock inlets

2.2.2 The External Compression Inlet with One or More Oblique Shocks Followed by a Normal Shock

External compression inlets produce system of oblique shock waves external to the inlet, to reduce the Mach number from the free-stream value and followed by a normal shock at or near the cowl lip through which the flow becomes subsonic [5]. This arrangement is shown schematically in Figure2.7(a) for the simplest (two-shock) external compression inlet and Figure 2.7(b) illustrates a typical three-shock external compression inlet. Oswatitsch [6] first demonstrated the effectiveness of external compression inlets, and Ferri and Nucci first presented analytical and experimental studies of such inlets [7]. Discussion of these inlets is presented by Seddon and Goldsmith [8]. Design aspects of various inlets were analyzed in some detail by

Connors and Meyer [9]. An interactive design tool for external compression inlets is described by Benson [10].

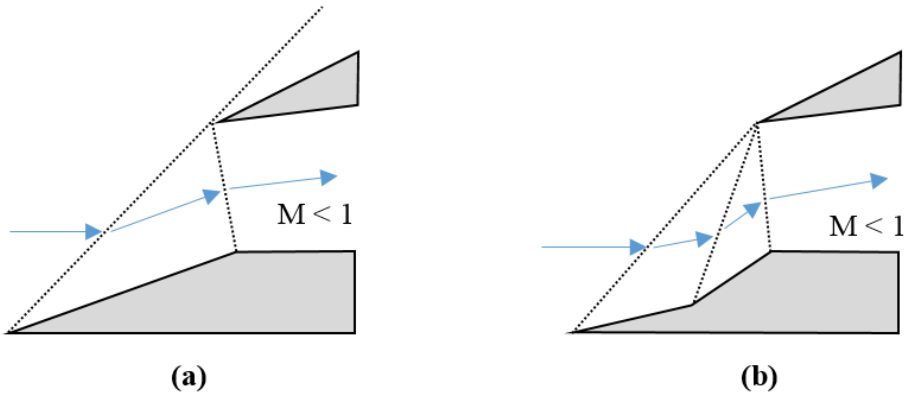

Figure 2.7: Schematic diagram of two type of external compression inlets (a) External compression inlet incorporating two shock waves, (b) External compression inlet incorporating three shock waves

The total pressure recovery for external compression inlets with oblique shocks of equal strength followed by a normal shock is presented in Figure 2.8 as a function of free-stream Mach number. Increasing the number of oblique shocks increases total pressure recovery for any given free-stream Mach number.

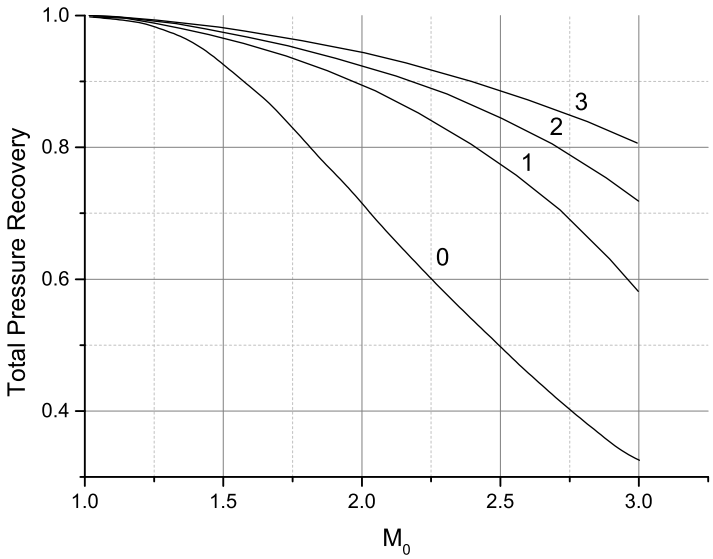

Figure 2.8: Total pressure recovery for external compression inlets with *n* oblique shocks

The ramp of the external compression inlet turns the flow away from the axial direction. This air must be captured and turned by the inlet cowl lip back to the free-stream direction which may not be possible without separation. Also, large lip angles

are required to capture the flow but that gives rise to an additional source of drag (cowl drag). Increasing the free-stream Mach number, increases the cowl drag and diminishes the net performance of the inlet. Figure 2.9 shows the total turning angle of an external compression shock system that attains the total pressure recovery of MIL − E − 5008B as a function of free-stream Mach number [11].

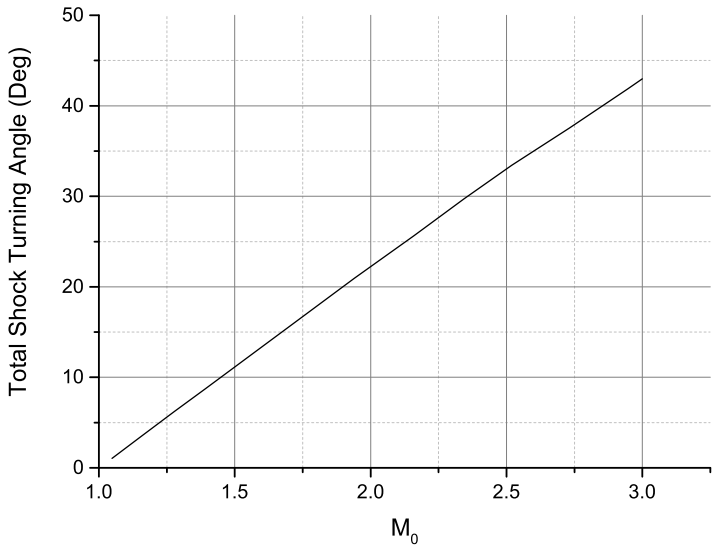

Figure 2.9: Turning angle of external compression shock system

2.3 Mixed Compression Inlets

The mixed compression inlet uses both external and internal compression before the terminal normal shock in order to relieve the cowl drag problem. At flight Mach numbers above 2.5, the mixed compression inlet is used to obtain an acceptable total pressure ratio while obtaining acceptable cowl drag. For example, at a flight Mach number of $M_0 = 3$ a four-shock external compression inlet and a mixed compression inlet are shown in Figure2.10. At external compression case the flow turns approximately 40^o up from the horizontal therefore, the cowl lip would have to be at an angle of at least that amount to capture the flow. However, at mixed compression case some of the compression takes place downstream of the cowl lip with the interior of the cowl providing suitable flow deflections, as a consequence the angle of the cowl lip is much reduced, likewise cowl drag, as shown in Figure2.10(b). Nevertheless the mixed compression inlet is more complex, heavier, and costlier than the external compression inlet.

The ideal location of the normal shock is just downstream of the inlet throat, to minimize total pressure loss while maintaining a stable operating location of this shock. Similar to the internal compression inlet, the mixed compression inlet requires both fast-reacting bypass doors to maintain the normal shock in a stable location and variable throat area to allow the inlet to start by swallowing the normal shock [1].

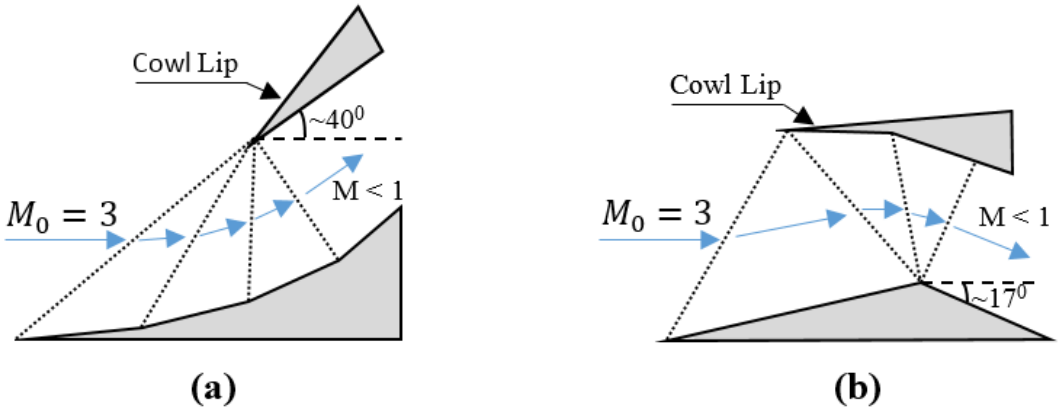

Figure 2.10: Schematic diagram of a four-shock external compression inlet and a mixed compression inlet at a flight Mach number of $M_0 = 3$ (a) Necessary flow deflections for a four-shock external compression inlet, (b) Necessary flow deflections for a mixed compression inlet

A problem that can occur in external compression and mixed compression inlets is called inlet buzz. Buzz is a low-frequency, high-amplitude pressure oscillation that is linked to shock/boundary layer and shock/shock interaction at relatively low inlet mass flow ratio. This instability in inlet operation may arise when the inlet is operating in a subcritical mode under reduced mass flow conditions. The main effect is rapid movement of the shock wave train in and out of the inlet itself, subjecting it to rapidly varying pressure and acoustic loads, which can compromise the structural integrity of the inlet. A detailed discussion of this phenomenon is given by Seddon and Goldsmith [8].

Comparisons of maximum range achievable in supersonic cruise using inlets with various degrees of internal compression from 0% (all external compression) to 80% internal compression show a decided edge toward those with a high degree of internal compression, according to Bowditch et al [12]. However, such inlets are sensitive to flow disturbances caused by gusts and maneuvers and are susceptible to inlet unstarts, where the swallowed terminal (normal) shock moves out of the inlet severely, reducing

the pressure recovery of the inlet, as described in Ferri and Nucci [7]. Throat bypass bleed systems can reduce this sensitivity but add weight and complexity to the engine. Lower performance inlets, like all external compression inlets, constitute a viable alternative to the airplane designer. A design approach for fixed geometry, mixed compression inlets has been proposed by Creta and Valorani [13].

3. EXPERIMENTAL SETUP

All experiments were performed in the 150 x 150 Trisonic Wind Tunnel, located at the Trisonic Research Laboratory (TAL) of Istanbul Technical University. This chapter presents basic descriptions of the wind tunnel, the model and the instrumentation, which were used in the experiments.

3.1 Wind Tunnel

The Trisonic Wind Tunnel is a blowdown type wind tunnel with a test section area of 150 mm x 150 mm and a length of 400 mm, and can operate at Mach number ranges of 0.4 - 2.2 (with the liner module) and 2.4 - 4.0 (with the blocks module) by using two different test-section/nozzle modules. However, since the lower Mach number (0.4 - 2.2) test section had larger glass side walls for imaging, and it was possible to modify and arrange the test section floor for model mounting this test section was used for the experiments. The schematic layout of the wind tunnel and the auxiliary equipment can be seen in Figure 3.1.

The trisonic wind tunnel is supplied with air from two high pressure tanks of 45 m^3 each which are filled using a two-stage compressor system. The starting point of the compressing process is the 10-Bar Compressor (1). First, air is compressed to about 10 bars in this first stage compressor and stored at the 10-Bar Tank (2). This first stage compressed air is then sent to the refrigeration dryer (3) after passing through a filter. Refrigeration dryer provides a preliminary stage in decreasing the humidity of the compressed air, which condenses and evacuates the water molecules in the air by cooling. The process is followed by re-filtering and transferring the air to final compression stage. A rotary screw-type high pressure compressor (4) receives the compressed air at 10 bars and compresses it up to 40 bars. During this second stage compression process, the temperature of the air increases significantly to levels above the working range(-10 to 60^{o}C) of the high pressure desiccant dryer (6) which is at the next station. In order to reduce the inlet temperature of the desiccant dryer,

a heat exchanger (5) which has a simple radiator mechanism with a cooling fan is used. The desiccant dryer operates by the principle of adsorption. Adsorption is a physical process that leads to the fixing of certain gas molecules (in our case water vapor) on the surface of solids materials called adsorbents or sorbents. The adsorbents are porous products and commonly have specific surfaces 500-1000 square meters per gram. This process is highly efficient, since the materials are easily regenerated for adsorption after reaching its saturation. Regeneration (also called reactivation) of materials for adsorption is the removal or evaporation of water adsorbed from the same compressed air. This regeneration can be achieved by "washing" of the adsorption material saturated with dry air. To keep the pressure within the working range (35 to 40 bars) a high-pressure tank (7) is used with a check valve at its exit. Ultimately compressed air is stored at up to 40 bars in two identical pressure tanks (8) with internal volumes of 40 m^3 each. One pneumatically controlled and two manually operated isolating valves separate the tanks from the wind tunnel. Pneumatically controlled isolation valve (9) is actuated by the operator and computer according to safety pressure transducers and is essential in cases of emergency and unexpected pressure rise in the stagnation chamber of the wind tunnel.

An axially-controlled regulation valve (10), which is located at the inlet of the stagnation chamber (11), maintains the stagnation pressure within a range suitable for the experiment conditions. Furthermore, it is designed to provide a streamlined flow path and reduce high local velocities, turbulence and impacts of flow jets. In the experiments, the maximum opening and closing durations of the regulation valve are set to remain within 6 and 7 seconds.

Pressure is maintained at generally a constant value in the stagnation chamber to provide stable flow conditions in the test section. Stagnation chamber is the place where the static pressure is at the highest value along the entire upstream section of the tunnel after the regulation valve thus contains the safety systems. Therefore there is a pressure transducer installed to the stagnation chamber for each test-section / nozzle module that sends a signal to the control computer to close the pneumatically-controlled isolation valve in case of overpressurizing the stagnation chamber and subsequently further downstream sections of the tunnel. Each test-section / nozzle module also has a security membrane (12) placed in a corresponding chimney

on top of the stagnation chamber if the isolation valve takes too long or fails to close in case of overpressure. The membrane is designed to rapture and releave the internal pressure at and above 5 bars and 14 bars at 20^{o}C for liner and blocks modules, respectively.

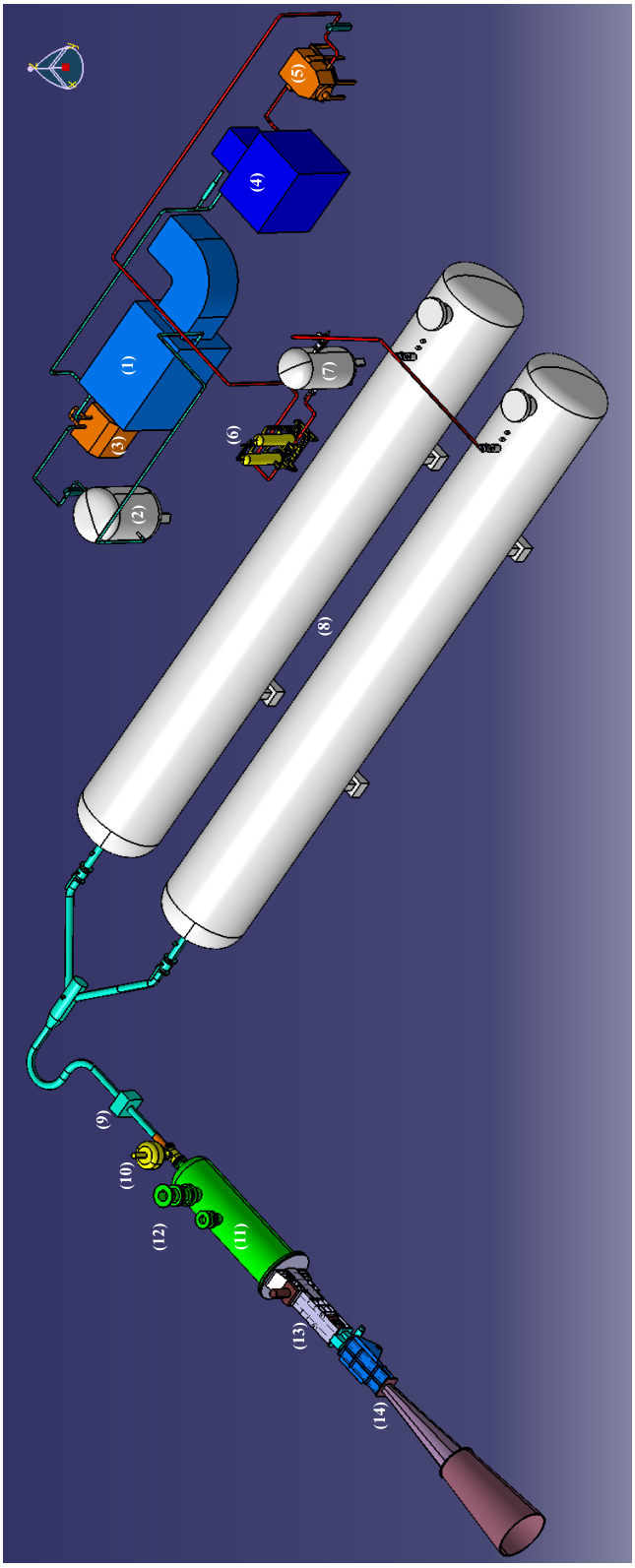

Figure 3.1: The schematic layout of the wind tunnel and the auxiliary equipment.

The liner test section/nozzle module which provides Mach numbers 0.4 - 2.0 used in the experiments (13). This test section module is 1.960 m long and it includes an adjustable first throat. The first throat is bounded by the two side walls 150 mm apart and by upper and lower walls converging down to the test section and thus varying the Mach number. The liners, which are used to change the throat area, are 1033 mm long and they are made of a lightweight alloy machined with a precision of 5/100 mm on definitive dimensions. A motorized mechanism is used to control the displacement of liners. Facing the model location, the side walls of the test section are equipped with 210 mm diameter round portholes fitted with Schlieren-quality glass windows. The portholes are mounted on hinges with a sealing and locking system. At the test section portion of the module each upper and lower wall has a boundary layer suction device. However, boundary layer suction device at the lower wall was removed in previous studies and this part of the test section floor was modified to be able to mount the inlet models on the floor. In addition to this modification, a brass plug with 35 holes for mounting the transducers flush with the surface at minimum 5 mm intervals was produced in order to perform the pressure measurements. Thus, a row of six fast-response transducers would be mounted using any six of these 35 ports at a time.

Finally air flow enters the diffuser (14) after test section portion of the wind tunnel. In the diffuser, flow is decelerated and exhausted to the atmosphere.

3.1.1 Data Acquisition System

The Trisonic Wind Tunnel has a 16-channel data acquisition system for the basic operation and measurements during the tunnel run. Data acquisition system also provides analog and digital outputs for controlling the valves and switches of the wind tunnel system. Operation of the wind tunnel, including controlling of the valves and throat mechanism, is performed via a FORTRAN program running on a computer (PC-1). During the operation of the tunnel, characteristic parameters (tank pressure, stagnation chamber temperature, total pressure and static pressure) are simultaneously recorded and displayed with the use of an in-house LabView code by another computer (PC-2) which is equipped with a data acquisition card (National Instruments DAQ PCI-6014). For the measurement of fluctuating pressures the transducer signals were sampled at a rate of 200 kHz with two A/D cards (National Instruments DAQ

PCI-6110E) installed in another computer (PC-3). The A/D cards are controlled by a LabView code. This allows acquiring and recording the time history of pressures in and around the model simultaneously during the experiments.

3.1.2 Schilieren System

The optical method used for flow visualization is the Schlieren technique and a scematics of the setup is shown in Figure 3.2. This system gives an image representative of the variation of density throughout the complete flow field of the test section. Light from a point source is collected into a parallel beam and passes through the wind tunnel test section. The parallel beam is then focused on a horizontal or vertical knife edge and used to create an image on a screen. Schlieren images were obtained from the videos recorded by using a high quality standard video camera.

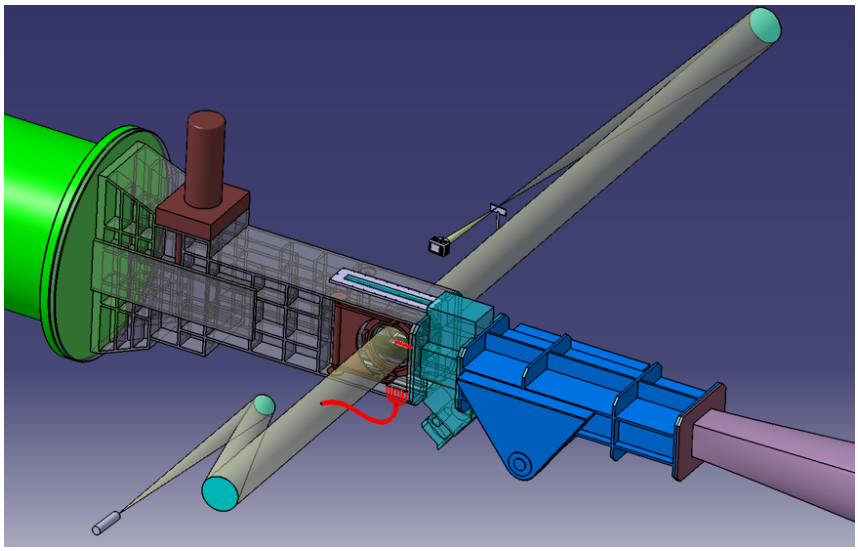

Figure 3.2: Schlieren set up of the Trisonic Wind Tunnel

3.2 Model

The inlet-isolator model was mounted on the floor of the test section as shown in Figure 3.3. The inlet portion of the model consisted of a 12-deg compression ramp. The inlet entrance height H_0 and the throat height at the entrance of the isolator h were 58 mm and 50 mm, respectively. The isolator and inlet were 137.4 mm and 37.6 mm long, respectively. The inner width of the model was 44 mm giving an inlet entrance aspect ratio of 0.76 and an isolator aspect ratio of 0.88. Blockage ratio of the inlet model was 5.5%. The model was a bolted assembly of four pieces. The upstream piece, made

of aluminum, contained the ramp and the isolator throat. The rest of the isolator was formed from an aluminum ceiling and two acrylic sidewalls to allow optical access. This resulted in a streamwise length of 143.1 mm where the flow within the inlet could be visualized. The thickness of the all three isolator pieces was 8 mm.

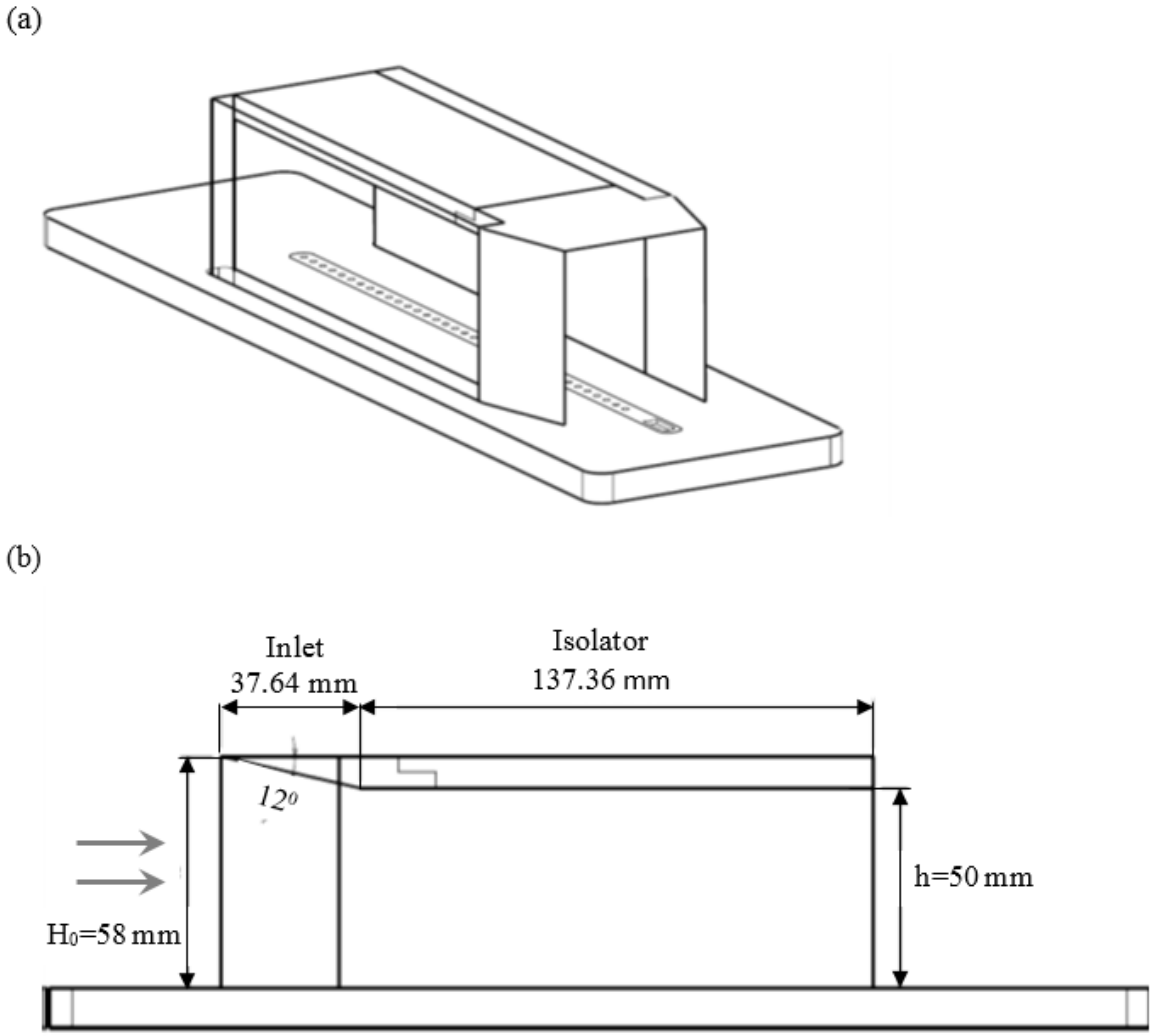

Figure 3.3: Schematics of the inlet-isolator model instrumented for simultaneous optical and pressure measurements.

3.3 Fast Response Kulite Pressure Transducers

A pressure transducer produces an electrical output proportional to the pressure applied. When pressure is applied, the force on the sensing element due to the pressure results in a deformation of the sensing element. This deformation changes the electrical properties of the element and the electrical output of the transducer. In a well-designed transducer, the deformation and electrical output are directly proportional to pressure

over a wide range of frequencies. The frequency of pressure fluctuation should be lower than the resonance frequency of the transducer and the electrical output is essentially independent of frequency below one-fifth the resonance frequency (flat frequency response).

In this study Kulite brand transducers (three of XCLE-072-50A, two of XCEL-072-25A and one of LQ-125-15A) (Figure 3.4 [14]) were used owing to their satisfactory performance at dynamic pressure measurements. The small size of these devices has also made them preferable because of large variety of test and production applications in research and development. These transducers have also found wide acceptance in the aerospace and the automobile industry, for wind tunnel, flight/road testing and acoustic measurements.

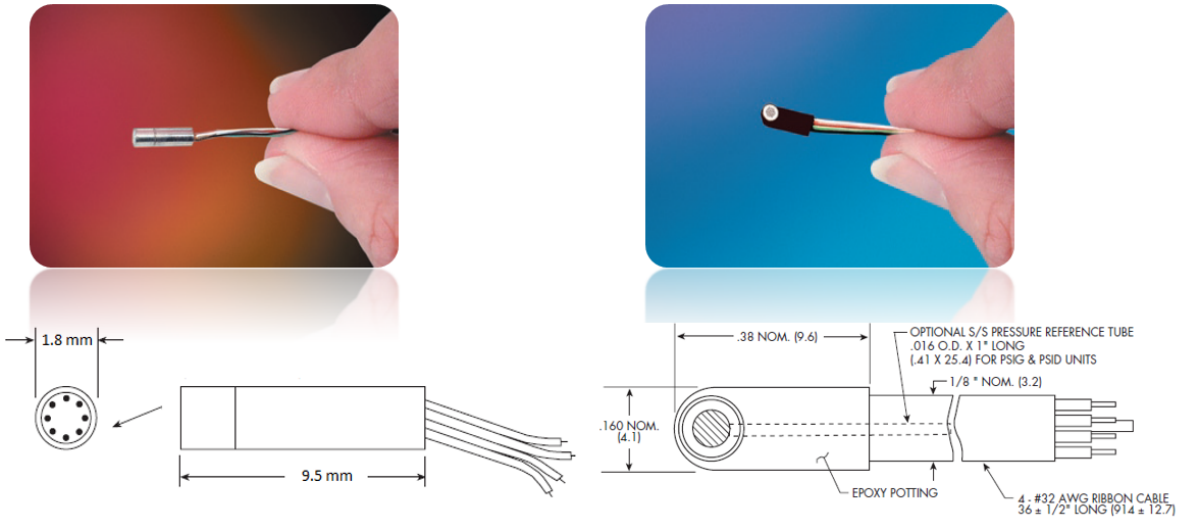

Figure 3.4: Kulite transducers that are used for dynamic pressure measurements.

Particular Kulite transducers that used in the study are not provided by the manufacturer with any sort of mounting means such as a screwing threads or a similar mechanism. As shown in Figure 3.5(a), special holder-sleeves with outer threads have been designed and manufactured both to protect the transducers from mechanical damage and to enable them to be re-installed in a given pressure port on the pressure plug. Transducers were placed and fixed securely in these sleeves with the use of nail polish and glue, so that they could be mounted in a given port and then moved to another port if needed. Ports without transducers were filled with blank plugs (Figure 3.5(c)) specially manufactured from standard screws to fit in these holes for isolating the flow within the inlet from conditions under the bottom of the tunnel floor.

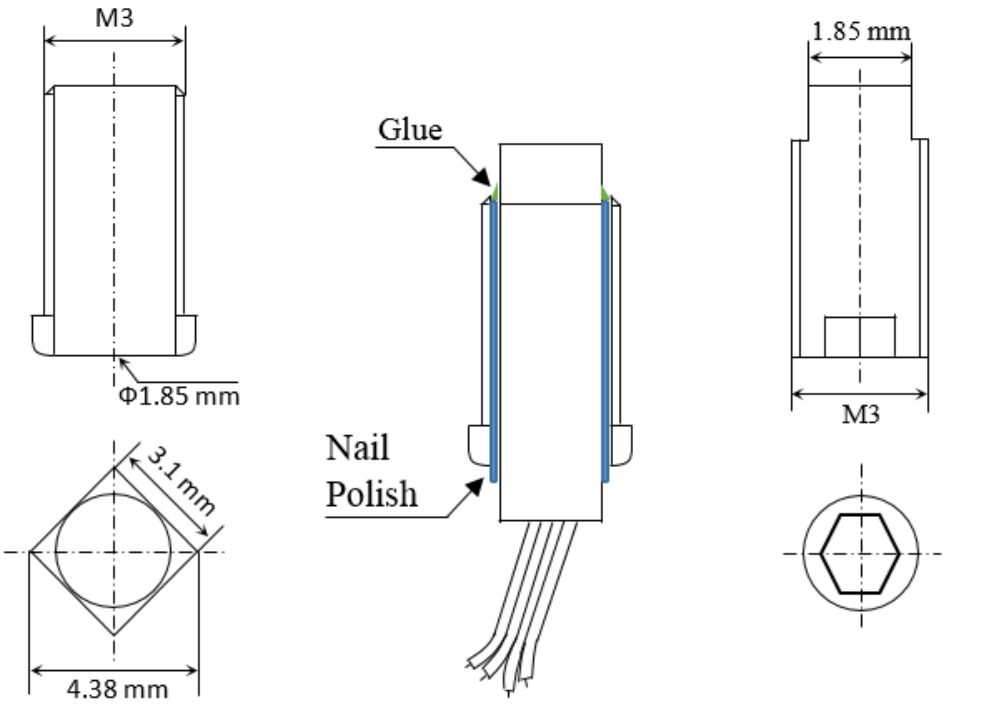

Figure 3.5: (a) Transducer Holder, (b) Transducer Assembled With The Holder, (c) Blank Plug

3.4 Calibration Unit

Transducers were calibrated for their output voltage in order to obtain the maximum signal resolution for data acquisition using the signal conditioning units which are provided by the manufacturer. For the calibration process, a vacuum/pressure box with provisions to supply a range of pressures was manufactured. As shown in 3.6, a vacuum pump (Value 1-Stage), an analog absolute pressure gauge (Wallace&Tiernan 1500 Series), a differential DC amplifier (Tesar-Electronic AW980-A4S), and a digital pneumatic calibrator (Wallace&Tiernan DPE750) were connected to the vacuum/pressure box. Using this setup, absolute pressures from 5 Pa to 345 kPa can be applied to pressure transducers placed in the box. The output signals corresponding to the applied pressure, amplified by the differential DC amplifier then sent to A/D card (National Instruments DAQ PCI-6110E). To perform the calibration and measurements

an in-house LabView code was developed and used. The calibration equation was obtained by the method of linear least squares.

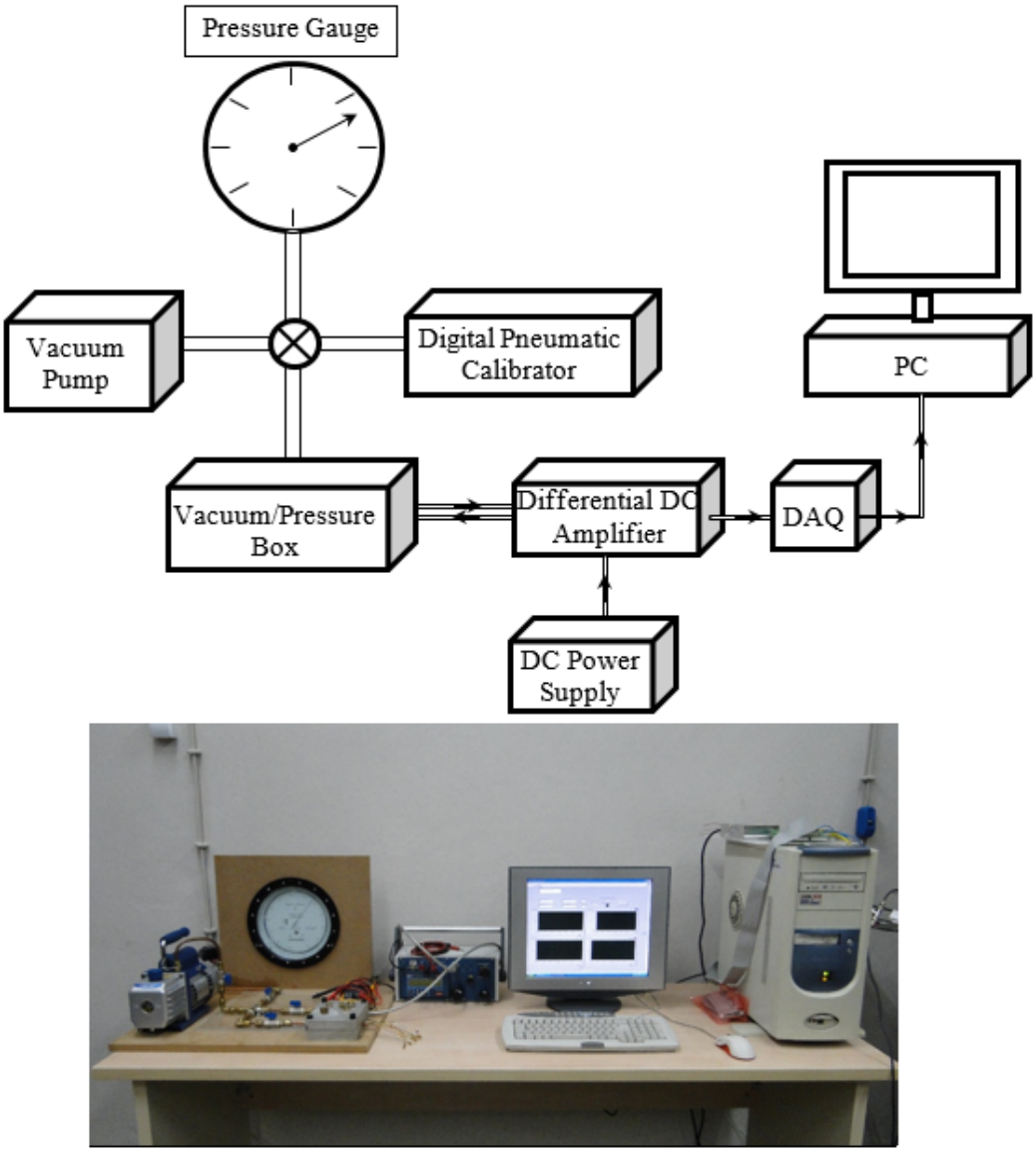

Figure 3.6: Schematic and the picture of the setup for calibration of pressure transducer.

4. RESULTS

Experiments were carried out in the Trisonic Wind Tunnel at Istanbul Technical University. About 70 runs were performed with the inlet model. Many of these runs involve the testing of the fluctuating pressure measurement system which was newly established. The runs for the actual pressure measurements performed after having demonstrated the reliability of the measurement system had essentially the same results for repeated runs at the same conditions. For this reason, results from the selected runs were presented here. Table 4.1 shows the conditions of the selected experiments.

Table 4.1: Test conditions

Experiment Number	T_0 [K]	$P_0 x 10^5$	Mach Number	U_∞ [m/s]	$Re_\infty x 10^7$ [1/m]
Run 2000	288.15	3.13	2.022	517.3	3.85
Run 2218	281.15	3.14	2.041	503.3	4.2
Run 2219	288.15	3.43	2.037	505	4.54
Run 2224	280.15	3.3	2.037	504.6	4.39

Figure 4.1 shows a schlieren image of the shock wave structure in and around the inlet taken during the run for a freestream Mach number of approximately 2. White lines mark the floor, 12-deg ramp, and the inlet ceiling. The inlet section is seen in shadow because they are made of aluminum. The initial oblique shock from the inlet ramp is seen as a dark line (arrow 1). The first reflected shock impinges on the inlet ceiling (arrow 2). The subsequent reflected shock is seen as a dark line (arrow 3), which then reflects again from the inlet floor (arrow 4). The initial shock wave generated by the inlet ramp and the reflected shock wave from the inlet ceiling impinge on the tunnel floor and interact with the relatively thick floor boundary layer at the locations shown by arrows *A* and *B*. Incidentally, two shock waves are generated at the point where the first reflected shock impinges on the inlet ceiling possibly due to the separation region formed by interaction with the ceiling boundary layer. These two shock waves apparently impinge on the floor in the region pointed by arrow *B*. This situation will be explained further in detail in the next sections.

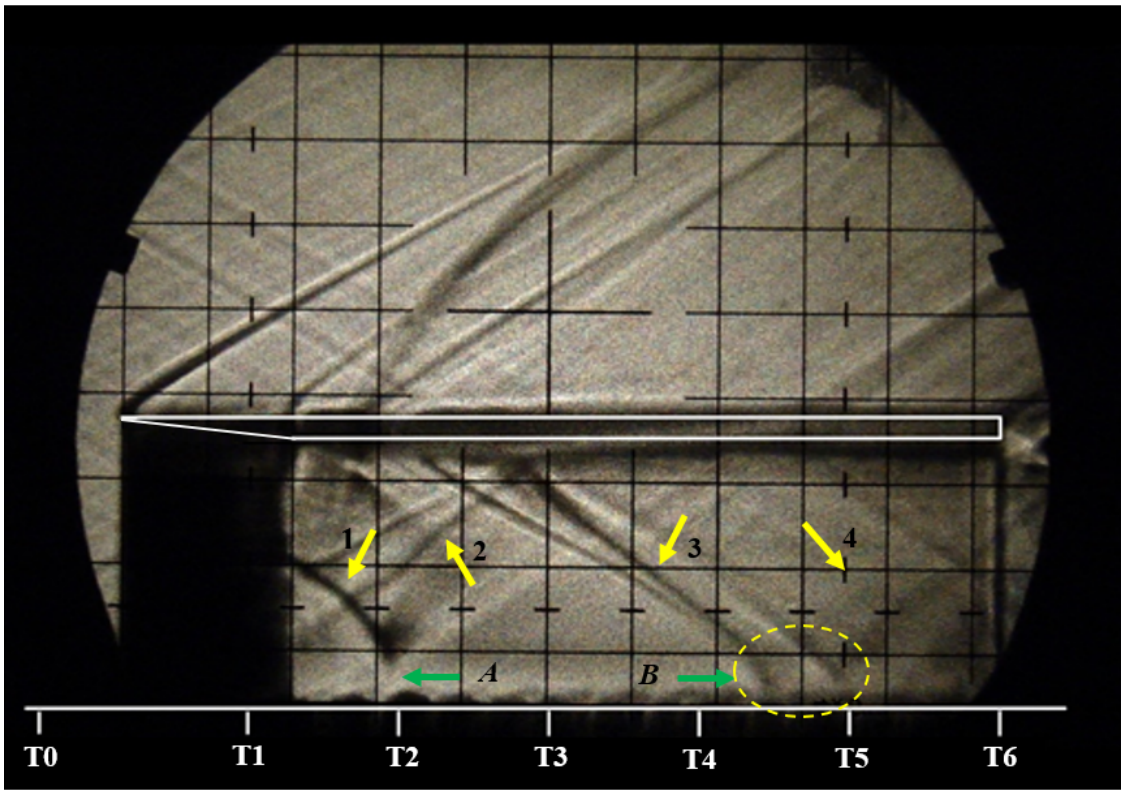

Figure 4.1: A sample schlieren image of flow in the inlet-isolator model at Mach 2.

Locations of the pressure transducers along the surface of the inlet floor for the pressure measurements were determined from the schlieren images. In the first case, transducers were installed at every six holes giving a 30 mm distance between them to obtain the overall pressure distribution along the floor of the inlet model. The time history of pressure data acquired at 200 kHz from all six transducers is shown in Figure 4.2 to indicate the general character of the pressure fluctuations for two different time periods, one for 2 seconds and the other for 10 milliseconds (Figure 4.2(a)). The pressure signal of each transducer is shown in separate graphs in Figure 4.2(b). From these separate pressure signals (Figure 4.2(b)) both the overall pressure history and the unsteady character for each measurement position can be seen more clearly. The fact that the magnitudes of the fluctuations in pressure signals at $T1 - T3$ seem to be considerably higher than downstream transducers ($T4 - T6$) and especially than the most upstream transducer ($T0$) indicates that the impingement of the ramp shock causes a strong interaction with the floor boundary layer.

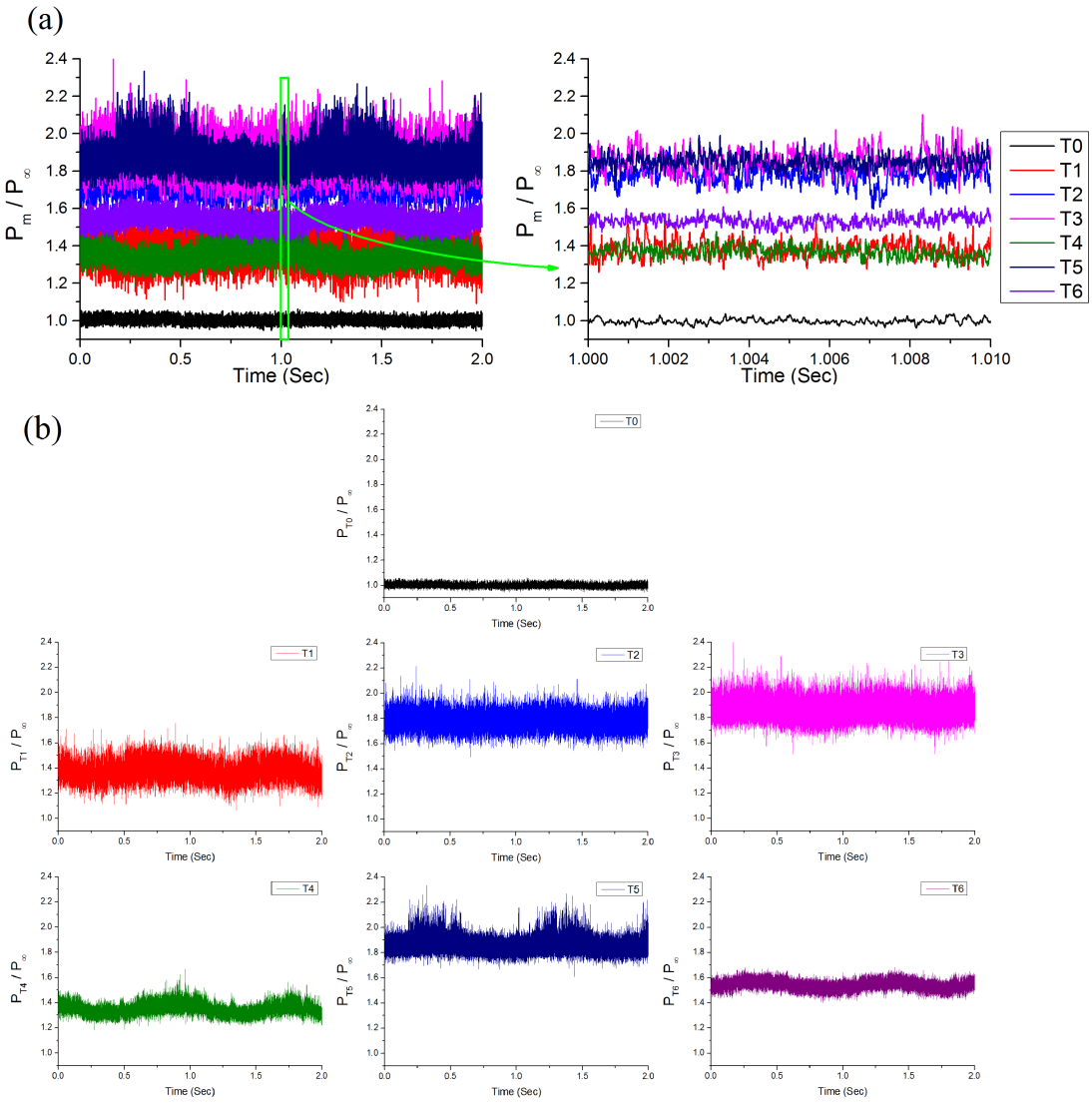

Figure 4.2: Pressure time history from Run2000; (a) Sample pressure signals from all transducers for time periods of 2 s (left) and 10 ms (right), (b) Individiual pressure signals of all transducers plotted separately.

From these measurements both the mean and rms of surface pressures were also obtained. The mean pressure P_m and the rms pressure σ_p distributions are shown in Figure 4.3. All pressures reported herein are normalized by that measured at transducer $T0$ since it provides a reference value that corresponds to that of the freestream. The pressure value measured at $T0$ remains essentially the same for cases with and without the model in the test section at the same Mach conditions. More specifically, the pressure at $T0$ was measured to be 37.1 kPa (5.38 psi) that is equal to the freestream pressure p_∞ at Mach 2 for the given run conditions. A representative schlieren image during the period at which the pressure data are taken is shown in Figure 4.3(a). Inlet

ramp, ceiling and the corresponding locations of the transducers on the floor are also shown schematically in Figure 4.3(a). Figure 4.3(b) shows that mean pressure has increased significantly along the wall from $T0$ ($x/h = -0.33$) upstream of the inlet to $T1$ ($x/h = 0.503$) within the inlet portion of the model due to the shock wave/boundary layer interaction occurring in that region. An additional pressure increase is seen at $T2$ ($x/h = 1.103$) and $T3$ ($x/h = 1.703$). At $T3$, the flow has been processed by the 12-deg ramp shock as well as the first reflected oblique shock. Using inviscid oblique shock theory, the pressure ratio of the free stream to that processed by two oblique shocks that form due to flow deflection angles of 12-deg is computed to be 1.86. The pressure ratio $P3/P1$, where $P1$ and $P3$ are the static pressures measured at transducers $T1$ and $T3$, respectively, is measured to be 1.866, which is in good agreement with the theoretical value. As the flow passes through reflections of the inlet shoulder expansion fan, the pressure decreases across $T4$ ($x/h = 2.303$). Moving downstream, at $T5$ ($x/h = 2.903$) the pressure increases back to about $1.8\,p_\infty$ for the same reason as $T2$. Finally the pressure decreases at the inlet exit near which T6 ($x/h = 3.503$) is mounted.

Figure 4.3(c) shows that $T1$ has the highest pressure fluctuations. Location of $T1$ corresponds to the upstream of ramp-shock impingement where the shock-boundary layer interaction occurs and therefore the resulting separated flow causes relatively large amplitude fluctuations. Fluctuations (rms) at $T3$ are also quite high. It may be attributed to the fact that $T3$ is downstream of two shock waves (ramp shock and the reflected shock) and thus turbulence levels in the boundary layer have been increased by these relatively unsteady shocks and the subsequent flow separation caused by the interaction. The amplitude of the pressure fluctuations generally decreases with the streamwise distance along the inlet.

In the second case, the transducers were moved to the entrance of the inlet where the initial oblique shock generated by the inlet ramp impinges on the inlet floor, and installed at every two holes giving a 10 mm distance between them. The time history of surface pressures sampled at 40 kHz from all six transducers is shown in Figure 4.4 for a time period of 10 seconds. Since it is somewhat difficult to distinguish individual signals when plotted on the same graph (Figure 4.4(a)), these pressure signals are also plotted separately to observe their general characters in Figure 4.4(b). As can be deduced from the signals all transducers within the inlet except $T1$ have a similar

general behavior. The pressure signal at $T1$ indicates that the mean value seems to have two different levels possibly caused by the back and forth motion of the separation shock foot in the interaction region upstream of the location around which the ramp shock impinges on the floor.

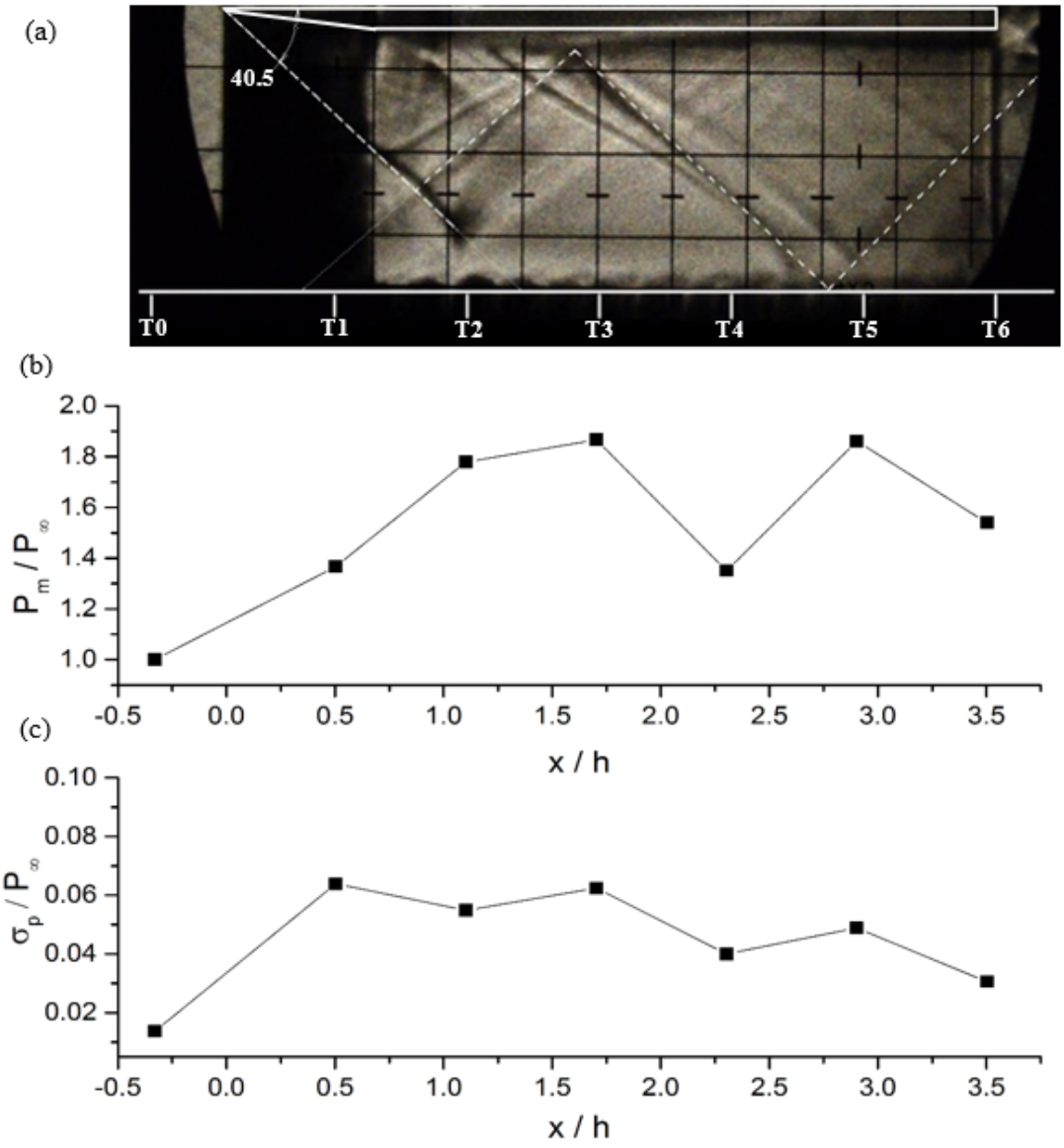

Figure 4.3: Results from Run2000; (a) A schlieren image, (b) Mean pressure distribution along the inlet/isolator model, (c) Standard deviation of pressure

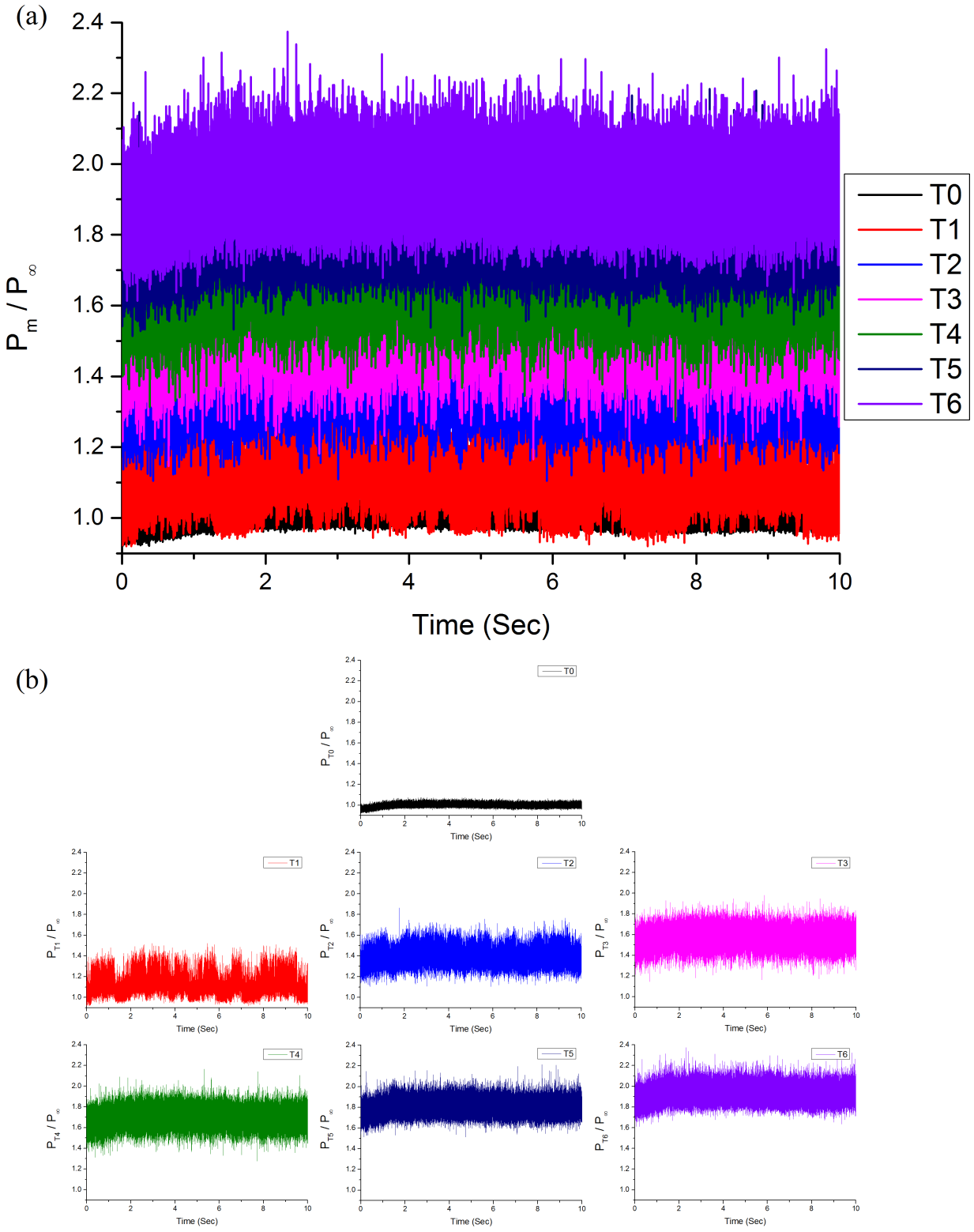

Figure 4.4: Sample pressure signals for a time period of 10 seconds (from Run2218); (a) All signals on the same graph, (b) each signal on a separate graph

A representative shadowgraph image taken during the period at which the pressure data are acquired is shown in Figure 4.5(a). The corresponding locations of the transducers

on the floor are also shown schematically in Figure 4.5(a). The mean pressure distribution shown in Figure 4.5(b) indicates that the pressure slightly increases along the wall from $T0$ ($x/h = -0.33$) upstream of the inlet to $T1$ ($x/h = 0.303$) within the entrance portion of the model. Furthermore, pressure increases significantly and constantly in the region from $T1$ ($x/h = 0.303$) to $T6$ ($x/h = 1.303$).

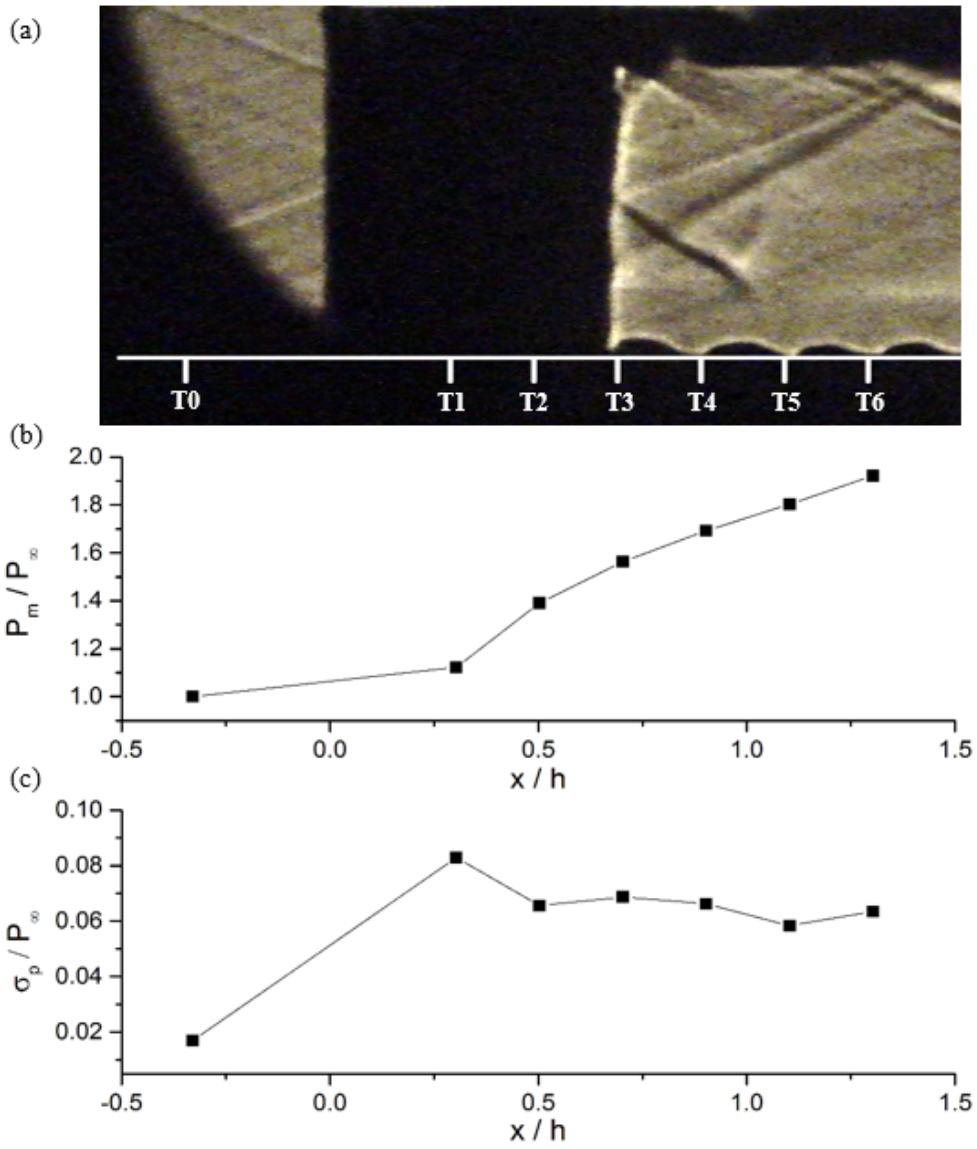

Figure 4.5: Results from Run2218; (a) A shadowgraph image, (b) Mean pressure distribution at the entrance of the inlet, (c) Standard deviation of pressure.

Figure 4.5(c) shows that the presence of the shock wave/boundary layer interaction in the region of ramp shock impingement has caused an increase in the rms of pressure fluctuations along the wall from $T0$ ($x/h = -0.33$) upstream of the inlet to $T1$ ($x/h = 0.303$). $T1$ has the highest pressure fluctuations among others. The

amplitude of the pressure fluctuations generally decreases after $T1$ ($x/h = 0.303$) to $T6$ ($x/h = 1.303$).

In addition, in the second case, transducers were moved further upstream to observe the pressure distribution between ($x/h = -0.33$) and ($x/h = 0.303$). Figure 4.6(a) shows a shadowgraph image taken during the period in which the pressure data are acquired in Run2219. Figure 4.6(b) shows that the $T1$ ($x/h = 0.103$) is located in the freestream region because pressure value is the same as that at $T0$ ($x/h = -0.33$). A slight increase is observed in the standard deviation of pressure at $T1$ ($x/h = 0.103$) in Figure 4.6(c). Based on this result it can be concluded that the separation region caused by the shock wave/boundary layer interaction begins immediately after $T1$ ($x/h = 0.103$).

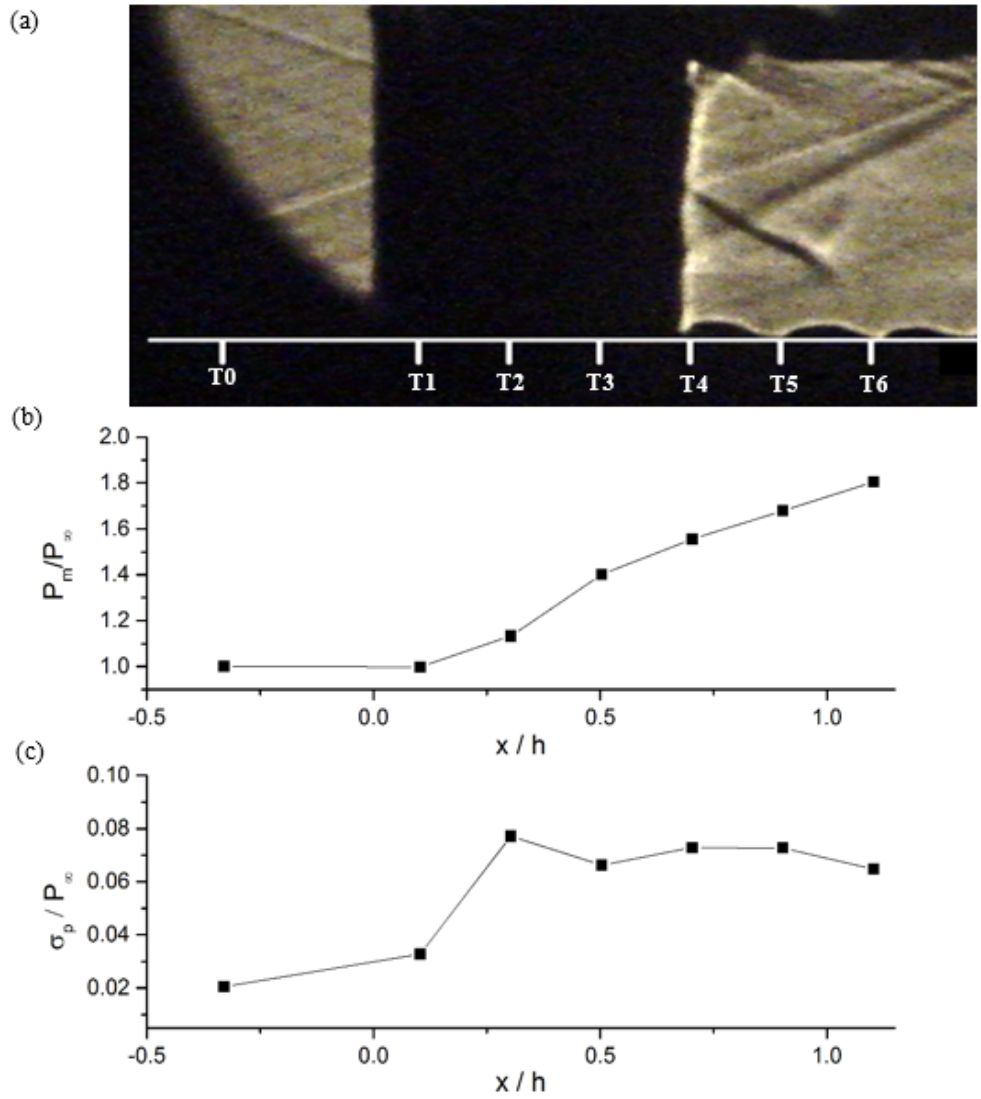

Figure 4.6: Run2219; (a) A shadowgraph image, (b) Mean pressure distribution at the entrance of the inlet, (c) Standard deviation of pressure.

In the third case, the transducers were moved further downstream of the inlet where the second reflected oblique shock impinges on the inlet floor. Transducers were installed at every hole in that region giving a 5 mm distance between them. The time history of pressure sampled at 40 kHz from all six transducers is shown in Figure 4.7 for a time period of 5 seconds.

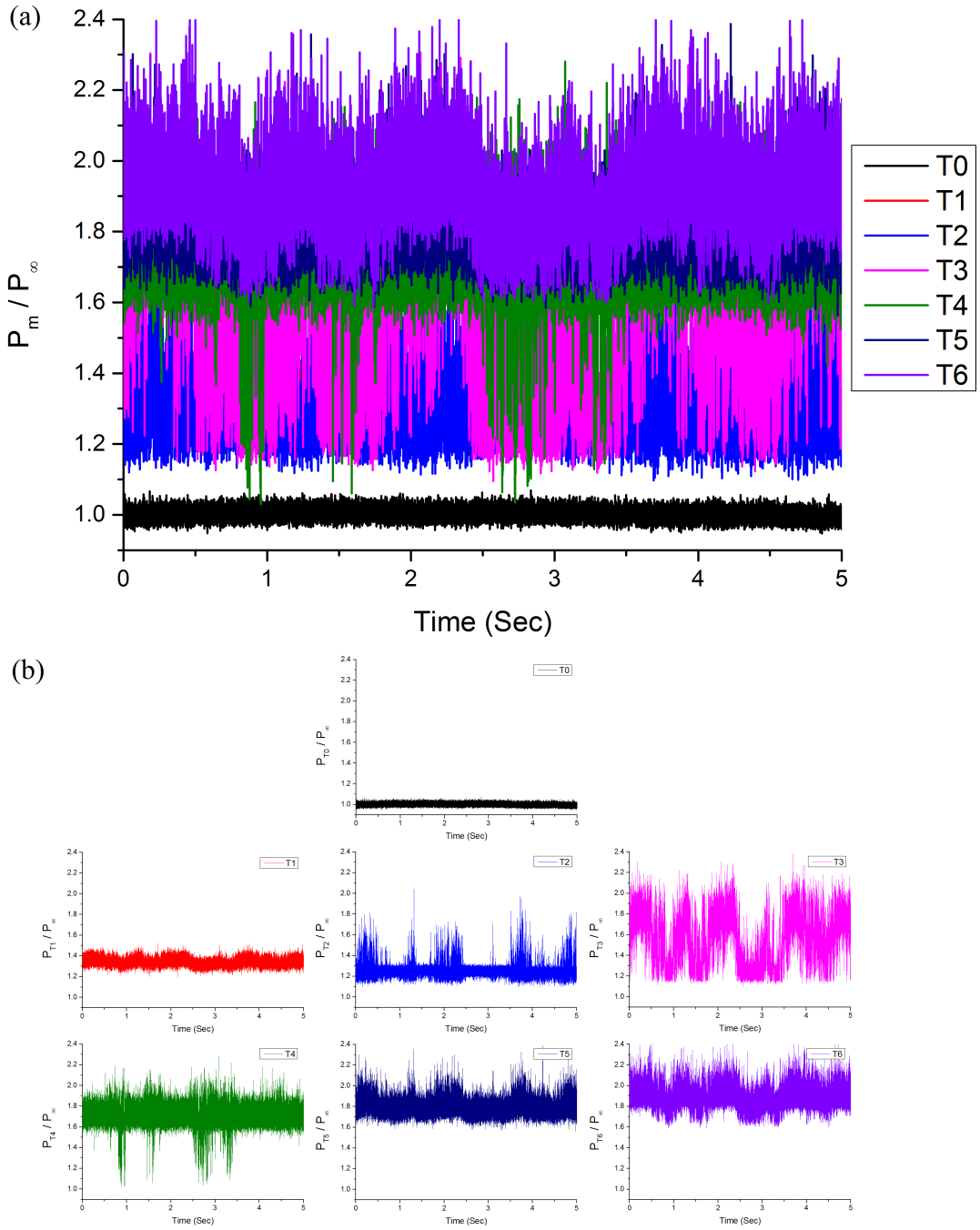

Figure 4.7: Sample pressure signals for a time period of 5 seconds (from Run2224); ((a) All signals on the same graph, (b) each signal on a separate graph.

Figure 4.8(a) shows that two oblique shocks, indicated by arrow 1 and arrow 2, are formed as the first reflection of the ramp shock impinges on the ceiling.

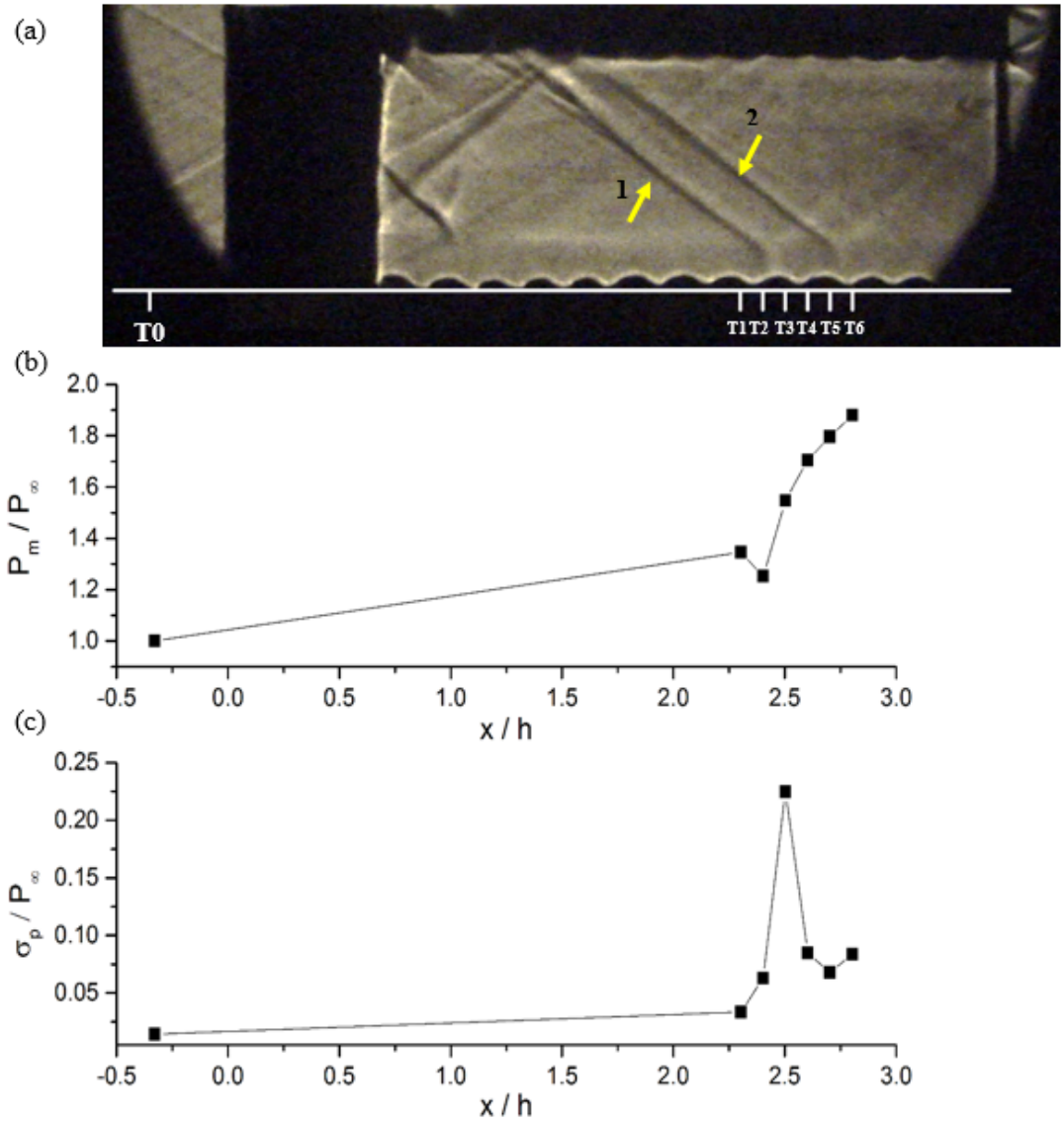

Figure 4.8: Results from Run2224; (a) A shadowgraph image, (b) Mean pressure distribution, (c) Standard deviation of pressure.

These two shocks seem to have been generated by the separation region formed due to the interaction of first reflected ramp shock with the ceiling boundary layer. The upstream one (marked by arrow 1) of the two shocks is the separation shock forming upstream of the local separation region due to deflection of the flow by the increased boundary layer and displacement thickness caused by the separation. The downstream one (marked by arrow 2) forms due to recompression caused by the expansion of the flow immediately downstream of the separation region. The pressure rise seen in Figure 4.8(b), which is caused by the upstream reflected shock is sensed first on

transducers $T3$ ($x/h = 2.503$). Downstream reflected shock appears to be impinging at a point between $T5$ and $T6$ ($x/h = 2.803$). Pressure increase caused by this shock may not be readily apparent in the mean pressure of T6 shown in the figure since this transducer can, at significant fraction of times, be upstream of the shock because of the unsteady behavior of these shocks which is evident both in pressure history shown in Figure 4.7 and also in the schlieren video (not shown in here) recorded during the run.

Figure 4.8(c) shows that $T3$ ($x/h = 2.503$) has the largest amplitude fluctuations because it is located at the point in between the upstream and the downstream reflected shock waves which are both highly unsteady and move slightly back and forth within this region.

REFERENCES

[1] **Mattingly, J.** (2006). *Elements of Propulsion: Gas Turbines And Rockets*, AIAA Education Series, American Institute of Aeronautics and Astronautics, http://books.google.com.tr/books?id=CuqHQgAACAAJ.

[2] **Raymer, D.** (2006). *Aircraft Design: A Conceptual Approach*, AIAA Education Series, American Institute of Aeronautics and Astronautics, http://books.google.com.tr/books?id=Uf2yQgAACAAJ.

[3] **Hesse, W. and Mumford, N.** (1964). *Jet propulsion for aerospace applications*, Pitman Pub. Corp., http://books.google.com.tr/books?id=8IFTAAAAMAAJ.

[4] **Antonatos, P.** (1972). *Inlet/Airplane Interference and Integration, AGARD Lecture Series No.53*, North Atlantic Treaty Organization Advisory Group For Aerospace Research and Development.

[5] **Sforza, P.** (2011). *Theory of Aerospace Propulsion*, Aerospace Engineering, Elsevier Science, http://books.google.com.tr/books?id=crYGWcPlIqAC.

[6] **Oswatitsch, K.** (1947). *Pressure Recovery for Missiles with Reaction Propulsion at High Supersonic Speeds: The Efficiency of Shock Diffusers*, NACA TM 1140.

[7] **Ferri, A. and Nucci, L.M.** (1954). *Theoretical and Experimental Analyses of Low-Drag Supersonic Inlets Having a Circular Cross Section and a Central Body at Mach Numbers of 3.30, 2.75, and 2.45*, NASA Technical Report 1189.

[8] **Seddon, J. and Goldsmith, E.** (1985). *Intake aerodynamics*, Aiaa Edu, American Institute of Aeronautics and Astronautics, http://books.google.com.tr/books?id=FnVTAAAAMAAJ.

[9] **Connors, J.F. and Meyer, R.C.** (1956). *Design Criteria for Axisymmetric and Two-Dimensional Supersonic Inlets and Exits*, National Advisory Comittee For Aeronautics (NACA) Technical Note 3589.

[10] **Benson, T.J.** (1994). *An Interactive Design and Educational Tool for Supersonic External Compression Inlets*, NASA-Lewis Research Center, TM 1066581.

[11] **MILE5008B** (1959). *Military Specifications for Engines, Aircraft, Turbojet Model*, NACA TM 1140.

[12] **Bowditch, D. N., C.R.E.S.B.W.S.N.E. and Wasserbauer, J.F.** (1971). *Supersonic cruise inlets. In Aircraft Propulsion*, NASA SP-259.

[13] **Creta, F. and Valorani, M.** (2002). *Optimal Shape Design of Supersonic, Mixed-Compression, Fixed-Geometry Air Intakes for SSTO Mission Profiles*, AIAA 2002-4133, 38th Joint Propulsion Conference, Indianapolis, IN.

[14] **Url-1**, (date retrieved 11.12.2013), `http://www.kulite.com`.

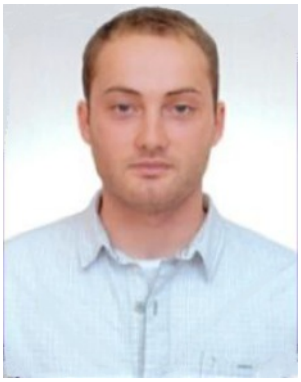

CURRICULUM VITAE

Name Surname: Hasan Tabanlı

Place and Date of Birth: 05.05.1985 Bulgaria

Adress: Istanbul Technical University, Faculty of Aeronautics and Astronautics, Trisonic Research Laboratuary Maslak, ISTANBUL

E-Mail: hasantabanli@itu.edu.tr

B.Sc.: Yıldız Technical University, Physics Department

List of Publications:

Tabanli, H., Yuceil, K. B. (2013): Fluctuating Pressure Measurements in a Inlet-isolator Model in Mach 2 Flow, 7th Ankara International Aerospace Conference, September, Turkey.

Tabanli, H., Acar, H. and Tasseven, C. (2009): Truck Aerodynamics: Device to Reduce the Drag Force, 7th International Student Conference of the Balkan Physical Union, September, Turkey.